Journal of Engineering Mathematics **48:** 187–217, 2004.

Slamming in marine applications

ODD M. FALTINSEN, †MAURIZIO LANDRINI[1] and MARILENA GRECO[1]
Centre for Ships and Ocean Structures, NTNU, N-7491 Trondheim, Norway; [1]*INSEAN, The Italian Ship Model Basin, Via di Vallerano 139, 00128 Roma, Italy*

Received 22 January 2003; accepted in revised form 1 August 2003

Abstract. Practical slamming problems for ships and ocean structures are briefly described. Theoretical status and future challenges for water entry on an initially calm free surface, wetdeck slamming, green water and sloshing are presented. It is emphasized that slamming should be considered in the framework of structural dynamics response and integrated with the global flow analysis around a ship or ocean structure or with violent fluid motion inside a tank. Two-phase flow can give important loading and needs to be better understood. Slamming on a VLFS with shallow draft is dealt with in detail.

Key words: free-surface flows, hydroelasticity, marine technology, numerical methods, slamming, two-phase flows

1. Introduction

Slamming is of concern in many marine applications. We will focus on ships and offshore structures. Slamming on ships is often categorized as bottom, bow-flare, bow-stem and wetdeck slamming. The wetdeck is the lowest part of the cross-structure connecting the two side-hulls of a catamaran. Wetdeck slamming has similarities with other nearly horizontal parts of a ship, such as large overhanging sterns. Green-water impact on deck structures and bow-stem slamming are of concern for Floating Production Storage and Offloading (FPSO) units, as sketched in Figure 1.

Wave-induced ship motions can cause violent fluid motion (*sloshing*) in partially filled tanks when either surge, sway, roll, pitch or yaw motions contain energy in the frequency domain close to the lowest natural frequency for the fluid motion in the tank. Violent fluid motions cause large slamming loads. Secondary impact on ship hulls due to separation should also be considered. An example is water entry of a bow characterized by large sonar domes. The jet-flow separating from the sonar dome can cause secondary impact on the hull. There are similarities between slamming on ships and offshore platforms. Breaking waves can impact on a ship hull or the columns of a platform. Run-up along the columns can cause local damage of the platform deck; see Figure 2. A platform is normally designed with an air gap to avoid global water impact. However, slamming may happen due to unanticipated large waves or due to subsidence of the sea floor for bottom-mounted platforms. Many offshore marine operations involve the lowering of objects through the free surface. Since the lowering velocity is small, the waves cause both water entry and exit. Examples on more special types of water impacts

†This paper is dedicated to the memory of Maurizio Landrini who died only 40 years old in a tragic motor-cycle accident. Still very young, he had made significant contributions to free-surface hydrodynamics and was this year selected to present the prestigious Weinblum lecture.

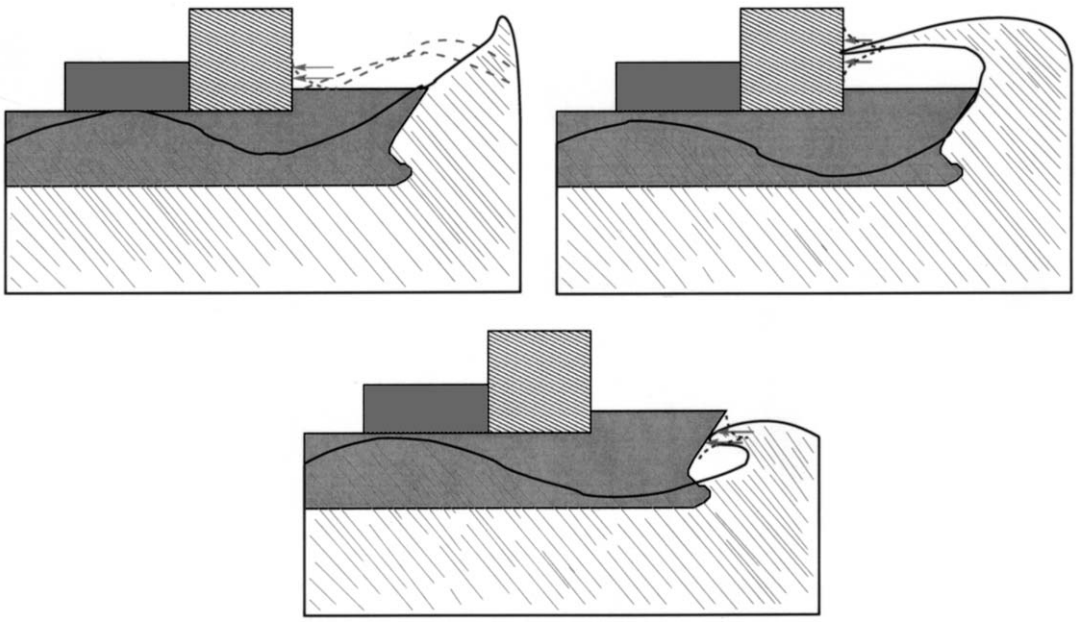

Figure 1. Green-water slamming on deck and bow-stem slamming.

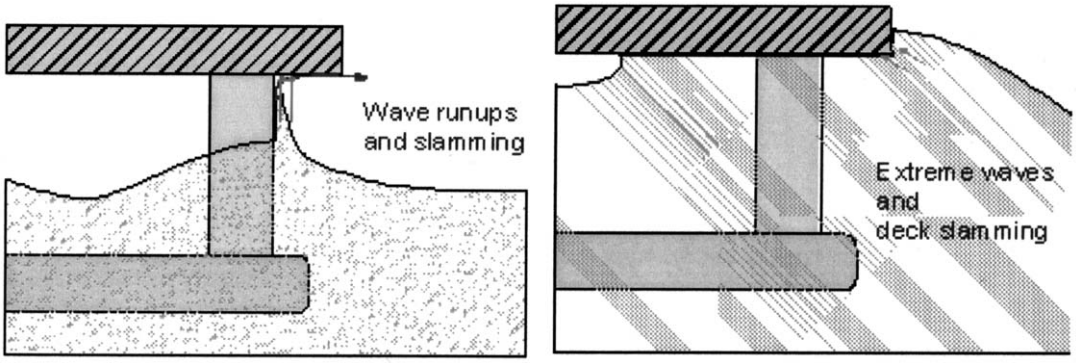

Figure 2. Left: wave run-up and slamming on deck platforms. Right: extreme-wave impact on deck platforms.

are slamming on air bags of air-cushion supported catamarans (Surface Effect Ship, SES), drops of mines, accidental drops of pipes from platforms and analysis of free-fall life boats.

Slamming is a complicated physical process where compressibility of the water, air cushions, air bubbles and hydroelasticity may be relevant. The practical relevance of these effects must be considered in the framework of structural-dynamics response. The time scales for structural response are associated with the natural periods of structural elastic and rigid-body vibrations. For example, if resulting maximum structural stresses due to wetdeck-catamaran slamming are focused on, a representative time scale of local wetdeck slamming is 10^{-2} s, while the time scale when global elastic effects matter is of order of 1 s. Here, the global effects refer to vessels of length larger than 50 m for which global longitudinal vertical bending has to be considered. Since the time scales of compressibility of the water, air cushions and air bubbles are typically much smaller, we may assume incompressible water and neglect the interaction between water and air in that context. However, we must be careful when

generalizing. In the main text, we will give examples where, for instance, an air cushion is formed as a consequence of waves plunging onto the deck and as a consequence of bottom impact on shallow-draft barge-type Very Large Floating Structure (VLFS). The air-cushion pressure matters in both cases. This implies that Froude scaling of model-test results cannot be used. Since significant viscous effects do not have time to develop during impacts, the flow can be assumed irrotational. If flow separation happens during the water-entry phase, like it does during the water entry of a sonar dome, this is not due to viscosity. The fluid acceleration associated with initial impact is generally much larger than the gravitational acceleration. If, in addition, the time duration of the water-entry and water-exit phases are small relative to typical wave periods, we may neglect gravity when evaluating slamming loads. However, considering the whole wetdeck of the platform being wetted requires consideration of gravity effects. The same may be true for water entry of bodies associated with flow separation. Slamming analysis of practical situations may require integrated analysis of the impact as well as the global flows. Green-water loading and bow-stem slamming are examples of this.

Numerical methods have to be used to deal with many practical slamming cases. However, experiments and analytically-oriented methods play an important role. The experimental visualization of the flow field can help in understanding how to model the flow theoretically. Examples on this related to how green water enters the deck in terms of a plunging breaker and what the body free surface intersection looks like during the water-exit phase of wetdeck slamming will be given in the main text. The flow observations led to the introduction of Kutta conditions in order to properly model the smooth detachment of the flow from the body. Analytically-oriented methods generally have the advantage of being more robust and time-efficient than methods that rely entirely on the Computational Fluid Dynamics (CFD). When the former methods are not available for modelling the whole flow, they may be useful in modelling local details within CFD-oriented methods. An example of this for bottom slamming on a barge-type VLFS will be given in the main text, where an analytical solution is used to describe the local flow when the angle between the impacting free surface and the body surface is small.

A more general comment is related to verification and validation of numerical methods. Analytically oriented methods and experiments obviously play an important role in this context.

The paper contains four main sections dealing with, respectively, water entry on an initially calm free surface, wetdeck slamming, green water and slamming, sloshing and slamming. Each section describes status and future challenges from a theoretical point of view. Slamming on a VLFS with shallow draft has been chosen to be dealt with in more detail.

2. Water entry on an initially calm free surface

2.1. STATUS

Common analysis assumes a rigid body, symmetric impact, incompressible fluid, irrotational flow, neglection of gravity, no air cushions and no flow separation. Methods are well established for two-dimensional flow conditions and used, for instance, to calculate slamming loads on ship hulls. Necessary relative vertical motions and velocities are obtained by neglecting the influence of water-entry loads on ship motions. The pioneering contributions by von Kármán [1] and by Wagner [2] assume implicitly small local deadrise angles. Deadrise angle means the angle between the body surface and the impacting free surface without accounting for the

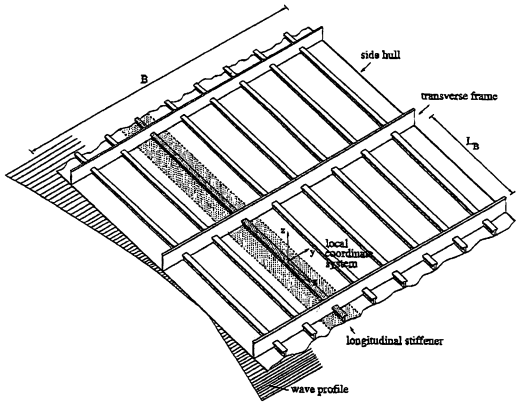

Figure 3. Part of wetdeck, The shaded part is included in the structural beam model, Haugen [20].

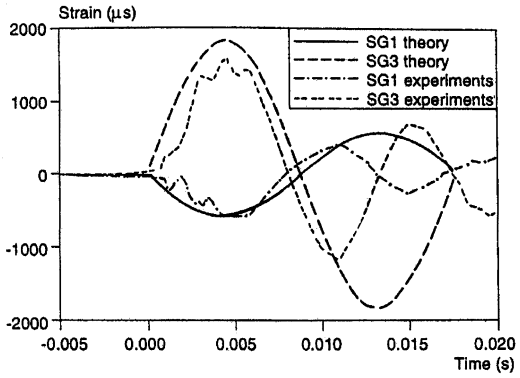

Figure 4. The strain at different locations along the beam as a function of time. SG3 is the middle longitudinal position of the beam. SG1 is close to one of the ends of the beam. Comparison between asymptotic theory and drop tests. Drop height is 0·5 m. Structural details given in Faltinsen [19].

influence of slamming. Since Wagner's method accounts for the local uprise of the water, it is more correct than von Kármán's method. However, we must realize that three-dimensional effects will reduce the loads and that after some time, for instance, gravity will affect the flow. Therefore we can not claim that in an integrated slamming analysis the use of the Wagner model gives a better result than that of von Kármán (*e.g.* the former could give too conservative force estimates than the latter). Wagner considered also the details of the flow at the spray roots. Cointe and Armand [3] demonstrated how this local solution can be matched to an outer flow. Cointe [4] analyzed also the body-attached jet-flow for a wedge and demonstrated the very small interior contact angle between body and free surface for small deadrise angles. Dobrovolskaya [5] provided a similarity solution for the symmetric water entry of a wedge with constant entry velocity and Zhao and Faltinsen [6] presented numerically similarity-solution results for a broad range of deadrise angles. Satisfactory comparisons were made with a Boundary Element Method (BEM) where the jet-flow was cut in order to obtain numerically stable solutions when the contact angle between body and free surface is small. The smaller the deadrise angle is, the more challenging the similarity and the BEM solutions are numerically. When the deadrise angle goes to zero, the results converge to Armand and Cointe's solution. An approximate and robust numerical method, referred to as 'Generalized Wagner method', was presented by Zhao *et al.* [7]. The exact body-boundary conditions in combination with approximate free-surface conditions used in the outer flow domain by Wagner were applied. Faltinsen [8] investigated how this solution matches with a spray-root solution for finite local deadrise angle. The results obtained by the Generalized Wagner method illustrate the importance of satisfying the exact body-boundary condition for finite deadrise angle, rather than transferring the condition to a flat plate like Wagner did.

The effect of compressible fluid has been extensively studied by Korobkin [9–13]. Air-cushion effects during the impact of a finite flat horizontal and rigid structure were examined by Verhagen [14]. This is initiated by the air-flow between the structure and the water be-

fore impact and when there is a small gap. Hydroelasticity relevance for steel and aluminum structures has been examined by Faltinsen [15] and by Korobkin and Khabakhpashewa [16]. A two-dimensional flow situation, where a horizontal structure is dropped on the free surface, is studied. The structure is represented by a beam model. The important parameter governing hydroelasticity is the ratio between the loading time and the highest natural period for the local structural vibrations in the impact area. If this ratio is sufficiently high, the structural response is quasi-steady. An analogy can be made to a simple mechanical system with a spring and a mass excited by an impulse load. This was systematically investigated by Faltinsen [17] for water entry of an elastic structure with a wedge-shaped cross-section of different deadrise angles β. By considering realistic structures, one could roughly state that hydroelasticity should be considered for $\beta < 5°$. When hydroelasticity is dominant, the impact pressures can be very high and concentrated in time and space during an initial phase. The physics of this phase was studied by Kvaalsvold and Faltinsen [18] and Korobkin and Khabakpashewa [16]. However, this detailed information has a small effect in predicting maximum structural stress. Further, fluid compressibility and air-cushion effects do not matter in general for maximum stresses. This was indirectly confirmed by Faltinsen [19] by comparing theory and experiments for impact of a flat horizontal plate on a free surface. However, the investigations by Haugen [20] suggest that air-cushion effects may be important when there are several dominant natural periods of structural vibrations. A three-beam model was used to represent the structure reported in Figure 3, consisting of a plating and longitudinal and transverse stiffeners. Transverse stiffeners are assumed rigid and the stiffened plating between two transverse stiffeners are made equivalent to a beam. When hydroelastic effects are dominant, *i.e.* $\beta \sim 0°$, and a one-beam model is considered, it is the force impulse during an initial stage in combination with structural inertia forces that matter. This causes a vibratory velocity of the structure with a space-averaged velocity that completely counteracts the rigid-body drop velocity. This initial velocity leads to a free elastic-vibration phase. It is during this free-vibration phase, after one quarter of the highest natural period, that maximum strains occur (see Figure 4). Later on, the free vibration will lead to negative pressure relative to atmospheric pressure. This occurs approximately when the strains at the middle longitudinal position SG3 in Figure 4 become negative. This can be explained by first noting that strains are proportional to the curvature of the beam which is directly related to the deformation of the beam. Assuming now a sinusoidal time dependence with the highest natural period of the beam, means that negative deformation corresponds to positive beam acceleration at the same longitudinal position. Since the fluid pressure at this stage is due to the beam vibrations, positive accelerations at SG3 will in general imply negative pressures at SG3. This can qualitatively be understood by considering a rigid body oscillating with a frequency and a vertical motion equal to the space-averaged beam deformations. This motion is closely related to the deformations at SG3. The fluid pressures cause the added-mass force which is negative when the acceleration is positive. The total pressure can be equal to vapor pressure, *i.e.* cavitation occurs. Since the submergence of the body is small, cavitation would lead to ventilation, therefore the structure starts to vibrate like in air. This is seen in the experimental time records presented in Figure 4. When the forward speed of the structure is high relative to the drop velocity, spray will only occur at the leading body-free surface intersection point. Faltinsen [19] analyzed this situation for the water entry of an elastic horizontal beam. An analogy was made to the unsteady flexible motions of a foil at small angle of attack. A Kutta condition requiring smooth detachment of the flow at the trailing body-free surface intersection point is then needed.

Flow separation from knuckles during water entry of a two-dimensional wedge was numerically studied by Zhao *et al.* [7] by neglecting the gravity. The solution approaches the steady cavity solution at zero cavitation number for flow past a wedge when time goes to infinity. These results were used by Zhao *et al.* [21] to find the steady vertical force and trim moment on a planing boat with a prismatic hull form. This was done by a $2\frac{1}{2}$D (or 2D+t) approach. This means that the flow in earth-fixed planes which the ship's longitudinal axis penetrates orthogonally, was studied. The problem in the earth-fixed planes is then for a general hull form the same as 2D water entry of a body with changing shape. de Divitiis and de Socio [22] studied unsymmetrical impact of wedges with constant velocity by means of a similarity solution. The symmetry axis of the wedge is vertical and the water entry-velocity has a horizontal component U and a vertical component V. Depending on the deadrise angle β and $\alpha = \tan^{-1} V/U$ the flow can separate from the wedge apex and be fully ventilated on the leeward side of the wedge. If $\beta > 45°$, the critical value α^* of α for separation to occur is very small, while $\alpha^* = 60°$ for $\beta = 7{\cdot}5°$. When the flow separates from the wedge, the problem is similar to water entry of a flat plate. The latter problem has been studied for small values of β and $90° - \alpha$ by Sedov [23] and Ulstein and Faltinsen [24].

All the previous cases refer to 2D flow. Classical axisymmetric water-entry studies are referred to by Miloh [25], who studied analytically water entry of a sphere. Faltinsen and Zhao [26] analyzed numerically spheres and cones. Scolan and Korobkin [27] examined theoretically 3D water entry of a rigid body in an incompressible fluid by making a Wagner type assumption, *i.e.* implicitly assuming small local deadrise angles and neglecting air cushions. The effect of flow separation for axisymmetric impact was investigated by Zhao and Faltinsen [28].

2.2. FUTURES CHALLENGES

Local hydroelastic effects on slamming has been dealt with in 2D-flow situations and for steel and aluminium structures for ships. One-beam and three-beam approximations of a stiffened plating have been made. The influence of a larger part of the structure should be examined. This may increase the number of eigenmodes that matter and would require a 3D-flow analysis due to the elastic deformations of a structure like that illustrated in Figure 3. The role of air cushions in this context should be dealt with. It is not clear if the findings for steel and aluminium structures can be generalized to composite structures.

Noise due to slamming, both in the water and within the structure, should be theoretically analyzed. Since this is associated with high-frequency vibrations of the structure in the impact area, it will require a much more detailed flow and structural analysis than required in assessing maximum structural stresses.

Another local hydroelastic slamming problem is impact of an air bag of a Surface Effect Ship (SES) in small sea states. The air bag is sealing off the major aft part of the air cushion created between two hulls of the SES in order to lift up the SES. There is a very small air gap between the air bag and the free surface in calm-water operating conditions. Slamming on the air bag changes the air volume inside the bag. This has a pumping effect on the flow in the air cushion between the two hulls. The concern is related to resonant air-flow conditions in the air cushion which can cause unpleasant vertical accelerations of the SES in small sea states. Both the water-entry and water-exit phases are believed to matter. The main structural deformations of the air bag are due to membrane effects. Since the forward speed of the SES is very high relative to the vertical impact velocity, the flow will separate smoothly from the

aft body-free surface intersection point. Ulstein [29] has analyzed this problem by considering a 2D hydroelastic problem and assuming a fixed given flow-separation point corresponding to the lowest point of the air bag in its steady configuration. More knowledge is needed about the air flow before impact, the separation point and the water-exit phase.

Not everything related to air cushions is understood. An air cushion may for instance be created in the initial phases of water entry of a blunt body, as a consequence of large deceleration of the body, due to flow separation accompanied by secondary impact or due to the local geometry of the impacting free surface. The closure of the air cushion is not clear in the first case. Further, how should we describe the flow in the air cushion? Sometimes only a constant pressure field dependent on the cavity volume and an adiabatic relationship between pressure and volume is used. It should be realized that air-cushion studies for a rigid structure may not be relevant for practical situations. A structure deforms more easily than water due to the air cushion pressure. There is also a scaling problem of model-test results. A parameter like $(p_a - p_v)/(\rho U^2)$, where p_a is the atmospheric pressure, p_v the vapour pressure, ρ the fluid density and U a characteristic flow velocity must be the same in model tests and full scale. The process of break down of air cushion into bubbles needs also to be better understood.

The effect of flow separation is another challenge which has already been mentioned partly. Another scenario is asymmetric water entry of a wedge with cross flow at the apex in a situation when a similarity solution does not apply. This is expected to always initially cause a ventilated area near the apex of the wedge. If one side of the wedge should be fully ventilated, depends both on the keel angle, deadrise angle and velocity direction of the body. If partial ventilation occurs initially, flow separation from the apex associated with viscosity will occur at a later stage. Flow separation occurring during water entry of a body without sharp corners is a particular challenge. The flow separation is not associated with viscosity. The time from initial impact is not sufficient for zero-shear stress to develop on the body surface. This is the conventional criterium for flow separation due to viscosity. The flow separation during water entry has similarities to cavity flows past a blunt body. Generalization of this to 3D impact situations like for the impact of accidentally dropped pipe from a platform is not clear.

When it comes to applicability to ship slamming, efforts should be made towards integrating the slamming analysis in the global flow description around the ship. This will properly account for the mutual interaction between slamming loads and global ship behaviour. This is for instance important for bow-flare slamming. Another case is for stern overhangs of a ship. This would require as a first step a nonlinear potential-flow model for an incompressible fluid where gravity effects are naturally included and exact nonlinear free-surface conditions are satisfied. Ideally viscous effects should be included to, for instance, properly account for viscous roll damping. Roll can have an important effect on slamming in oblique sea. However, solving the unsteady Navier-Stokes equations with proper free-surface conditions is still in its infancy. It is hard enough to solve a nonlinear potential-flow problem, governed by the Laplace equation. State-of-the-art nonlinear ship-motion codes simplify the free-surface conditions relative to what is used in water-entry analysis with nonlinear free-surface conditions. Since slamming loads can be sensitive to the angle between the impacting free surface and the body surface and depend on, for instance, the local three-dimensionality of the free surface, a procedure accounting for the mutual interaction between slamming loads and global effects of the ship can give a more realistic picture of slamming-load effects. When local hydroelasticity is important, the time scale of the local structure vibrations is very short relative to the time scale of the ship motion. This means that the structure can be considered locally rigid for a global analysis and local hydroelasticity can be dealt with separately. Global slamming

effects can cause important whipping, *i.e.* global transient elastic response of the ship. The resulting motions are not large but, since the frequency of whipping is high, it can play a role when calculating the relative impact velocity. However, there are sufficient challenges by considering the ship as rigid. One is to find properly the body-free surface intersection during water entry. The previously mentioned idealized water-entry studies for calm-water impact can provide important guidance. However, gravity as well as three-dimensionality of the flow will matter. When blunt-body impact occurs, the wetted surface changes very rapidly. This can be influenced by the local free-surface elevation due to the ship. It can be numerically difficult to deal with this situation. For instance, if we just consider a symmetric impact of a parabolic 2D rigid body on initially calm water, Wagner's theory gives that the rate of change with time of the wetted surface is initially infinite. A local analytical solution similar to Wagner's analysis can then be an effective mean to incorporate as a part of the global numerical method. Flow separation can also be an important scenario. An example is flow separation from a sonar dome. The resulting jet flow will most likely hit the structure and cause secondary impact. Another scenario is separation from the hull of the bow waves of a slender ship hull at high forward speed. This does not directly cause slamming loads, but must be dealt with in order to provide a robust global flow analysis of the ship. In a situation like this the bow waves will turn into plunging waves hitting the underlying free surface. Boundary Element Methods (BEM) cannot adequately handle this late stage of the impact of the plunging waves. Landrini *et al.* [30] have examined this problem by the Smoothed Particle Hydrodynamics (SPH) method. Even if this is a very robust numerical method, it is very time-consuming and it is at present not practical to apply for the whole flow domain. A domain-decomposition approach may then be needed where SPH is used for part of the flow. However, there are unsolved challenges as how to keep confined the particles within the SPH sub-domain. A pragmatic approach would be to disregard the effect of the plunging breaker and simply cut the jet like Zhao and Faltinsen [6] did for the water entry of 2D sections. When solving the problem fully integrated, water exit is another challenging part of the problem. This is less well understood theoretically than the water-entry problem. One has also the possibility of green water on deck. This is a problem that will be dealt with in more detail later. However, since bottom slamming for a ship at forward speed is most likely to occur in ballast conditions and green water is more likely to occur in full-load conditions, it is not always that we have to deal with slamming and green water simultaneously.

3. Wetdeck slamming

3.1. STATUS

Baarholm [31] studied global impact loads on a fixed and rigid horizontal wetdeck in incident regular waves and 2D-flow conditions. A BEM that accounts for gravity and nonlinearities in the free-surface conditions was used. This was combined with a Kutta condition at the aft intersection point between the deck and the free surface both when the flow separated from the aft edge and during the water-exit phase. In the present context, we define the water-exit phase as the period during which the wetted surface is decreasing. Experimental observations were the basis for applying the Kutta condition. Baarholm [31] demonstrated a good agreement between theoretical and experimental time histories of vertical force. The water-exit phase lasted much longer than a von Kármán method would predict. The water-exit phase causes a negative force. The maximum absolute value of the negative force is comparable to the

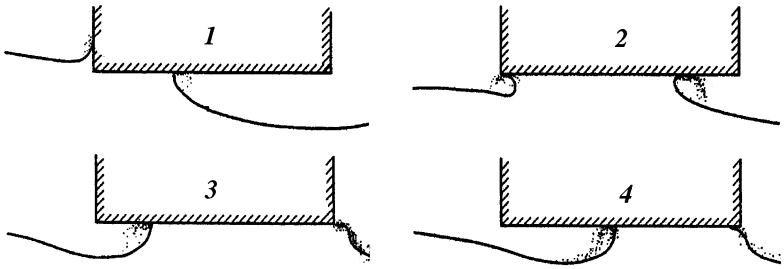

Figure 5. Experiments by Baarholm [31].

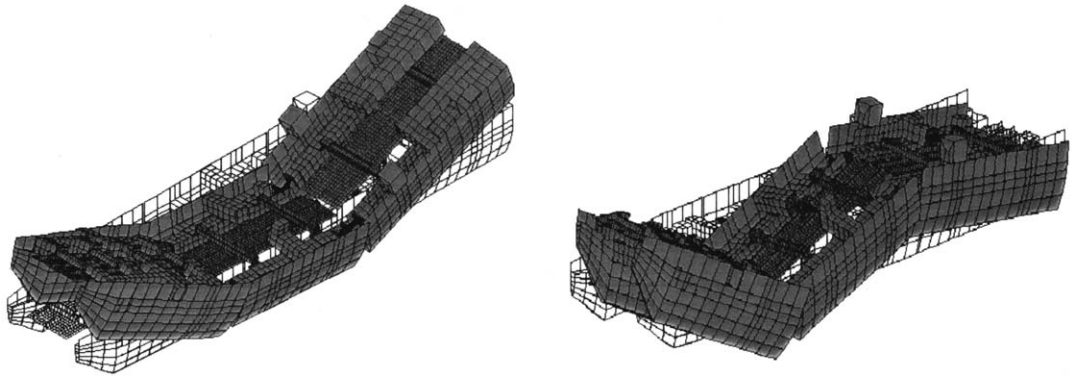

Figure 6. Calculated shapes of eigenmodes by Okland [34] for a catamaran consisting of three rigid body parts. Left: two-node longitudinal bending; right: three-node longitudinal bending.

maximum force during the water-entry phase. Figure 5 presents a schematic view based on video recording of the free-surface behaviour in Baarholm's experiments. The free surface hits initially at the front edge of the deck causing uprise of the water at the front end of the deck. The water will subsequently turn rapidly around the front edge with local high curvature of the free surface. This is probably amplified by a vortex created due to cross flow past the sharp edge. This rapid cross flow was artificially handled in the numerical method. The whole deck is subsequently wetted with the flow leaving the aft tangentially to the deck surface. When the wetted area later diminishes, there is smooth detachment from the aft body-water intersection point until final stages of the wetting. The free-surface slope is then high at the intersection point. The situation referred to above is the first impact event. If an impact has occurred during a previous wave period, the free surface in the deck area would be very different from the incident waves. This could cause multiple impacts on the deck.

It is worth mentioning that Baarholm's analysis is not intended to be of general applicability to any type of water exit encountered in hydrodynamics. For instance, during the emersion of a body initially fully submerged, depending on its speed, a certain amount of water is transported together with the body. The drying process in this case is rather different and probably significantly influenced by many other effects *(e.g.* the viscosity in the wake of the body, the surface tension during the drying phase).

Faltinsen [17] has studied local hydroelastic wetdeck slamming effects on the Ulstein Test Catamaran. The transverse cross-section of the wet deck contains a wedge-shaped part. The deck consists of a stiffened plating with longitudinal stiffeners between transverse frames. The transverse frames were assumed rigid in the analysis. The concern is maximum stresses in the longitudinal stiffeners. The hydroelastic theory was based on the orthotropic plate theory, strip

theory and a Wagner-type flow model in the transverse cross-sectional planes. Since the elastic deformation changes in the longitudinal direction, the rise-up of the flow will also change longitudinally. The relative inflow velocity was assumed vertical, space independent and time dependent. The results were compared with full scale tests in head-sea conditions where the measured slamming induced maximum local bending stress was close to half the yield stress. Reasonably good agreement was obtained but there were uncertainties in knowing what the time-dependent relative impact velocity was, during the experiments. The numerical results were sensitive to the time dependence of the relative inflow velocity. A reason is that relative inflow deceleration is large, the maximum stresses happen at the second lowest longitudinal stiffener and this occurs after the section touches the water surface. The initial impact did not occur close to the bow end of the wetdeck. If this had occurred, three-dimensionality of the flow would matter. Since the transverse cross section of the wetdeck had deadrise angles of 14° in the impact area, local hydroelasticity was not important.

Ge [32] has investigated theoretically and experimentally global effects of wetdeck slamming on a catamaran at forward speed in head-sea regular waves. The local structure can be considered rigid but global flexibility of the catamaran must be considered. The two-node and the three-node vertical modes are illustrated in Figure 6. The most important effect of wetdeck slamming was in terms of two-node vertical bending, but the effect on heave and pitch accelerations does also matter. There is a small but non-negligible effect due to three-node vertical bending. The focus was on vertical shear forces and bending moments along the ship. The global elasticity was modeled experimentally and theoretically by considering three rigid hull parts connected by elastic beam elements. The wetdeck had a bow ramp and was horizontal in the transverse direction. A slamming model with two-dimensional flow in the longitudinal section of the catamaran was used. This disregards the run-up along the hull sides. Since the slamming occurs at the front part of the deck and the conditions are head sea and non-zero forward speed, it is appropriate to assume the water elevation at most parts of the impact area is determined only by the incident waves. An important finding is that both the water-entry and water-exit phases are important for the global response. The details of how the forces were modelled were not so important for the global response. For instance, the sensitivity to using a Wagner model instead of a von Kármán model during the water-entry phase was not so important. Since a Wagner model can only be used during water entry, a von Kármán approach during water exit was combined with a Wagner model. The reason why a Wagner model fails during water exit is associated with the dynamic free-surface condition which assumes fluid accelerations to be dominant relative to gravitational accelerations. Mathematically this leads to the fact that no body-free surface intersection point can be found during water exit. Since a von Kármán model uses the same dynamic free-surface condition as the Wagner model, one can also argue physically against using a von Kármán model during water exit. However, a von Kármán model is based on geometrical intersection between body and undisturbed free surface. It will therefore provide a solution during the water exit phase. There is an important difference between Baarholm's and Ge's cases. The deck wetting in Ge's case lasts shorter than in Baarholm's. This means less importance of gravity. Ge neglected gravity when calculating the flow due to the impact and was able to show reasonable agreement between numerical and experimental slamming loads during the water-entry and water-exit phases. This includes also the duration of these phases. An experimental error analysis of the wetdeck-slamming-induced global vertical shear force (VSF) and bending moment (VBM) was made. An important error source is the steady trim angle of the vessel which is influenced by forward speed and wave-body interactions. The theoretical predictions of VSF and VBM

are reasonable relative to experiments. A major improvement is not expected to be due to the modelling of the slamming loads. It is more associated with how the hydrodynamic loads on the side hulls are modelled. The linear-frequency-domain strip theory by Salvesen *et al.* [33] without hull interaction was generalized to a flexible hull in Ge's studies. It was demonstrated that it is important to include the global hull flexibility in the slamming-load calculations.

3.2. FUTURE CHALLENGES

When it comes to offshore platforms, the work by Baarholm has to be generalized to three-dimensional cases. Experiments will then be useful in understanding how the Kutta condition should be applied. One reason for including 3D-flow effects is that inflow conditions will be three dimensional due to wave-diffraction and scattering effects of columns and other parts of the offshore platform. There is then also the possibility of several initial impact positions. However, even by disregarding these effects and assuming incident long-crested waves together with realistic deck dimensions, it is only during an initial phase that the flow can be considered as two dimensional. The flow is three dimensional when large negative forces occur. If we disregard the run-up along the columns, the inflow conditions are likely to be adequately described by state-of-the art computer tools, including possible second-order wave effects. The run-up along the columns can cause local damage of the deck. The description of the run-up is not state-of-the art. It should also be realized that the lower part of offshore platform decks facing the sea is not necessarily flat. There can be many stiffeners. This obviously complicates the slamming analysis. Both horizontal and vertical loads should be considered.

A major challenge for analysis of wetdeck-slamming-induced loads on catamaran or other types of multihull vessel is to adequately describe the side-hull hydrodynamics. Hull interaction is likely to be important. This cannot properly be described by strip theory. The steady flow should be analyzed in order to describe mean sinkage and trim at forward speed. Second-order wave-body interactions may also contribute to mean sinkage and trim. If linear wave effects for the moment are considered, a frequency-domain solution has inadequacies for global effects. The reason is that the wave-encounter frequency and the whipping frequency are very different. This can be properly handled by a time-domain solution. Nonlinear wave effects associated with the side hulls should also be considered. This actually leaves us in a situation previously described in Section 2.2. where slamming loads and global hydrodynamic flow should be simultaneously handled. However, assuming the inflow conditions are given, there are several scenarios where the slamming analysis has to be done by a 3D-flow analysis. This can be associated with the deck geometry that may have a non-flat transverse surface. Further oblique sea will cause 3D-flow situations.

Future challenges concerning local hydroelastic effects have implicitly been mentioned in Section 2. These should be extended by considering the local elastic structure integrated in the ship.

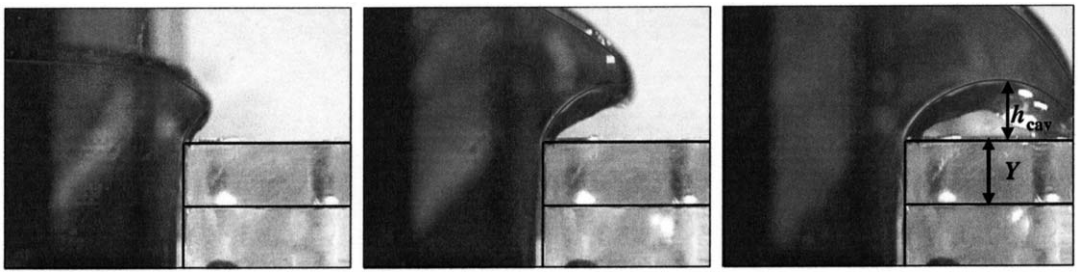

Figure 7. Initial stage of the water shipping. Numerical free surfaces (red lines) are superimposed to pictures from the experiment. The time interval between two snapshots is 0·04 s. Nominal regular incoming waves: $\lambda/D = 10{\cdot}1$, $H/\lambda = 0{\cdot}08$.

4. Green water and slamming

4.1. STATUS

Greco [35] has presented numerical and experimental studies for green water and slamming in a 2D-flow situation with incompressible water in irrotational motion. The body was restrained from moving and had nearly rectangular form with length-to-draft ratio $L/D = 7{\cdot}6$. The freeboard-to-draft ratio was $f/D = 0{\cdot}253$. A vertical wall was placed on the deck at a distance $d/D = 1{\cdot}15$. The set up has relevance for a FPSO in head-sea conditions and with a deck house in the forward part of the deck. Since ship motions influence green water, the freeboard was chosen to give realistic heights of the water over the deck at the bow. Regular incident waves of wave lengths relevant for green water were generated by a numerical wavemaker. Since it was focused on the first green-water event, the incident waves at the model were not regular at that time. A BEM satisfying the exact free-surface conditions was applied, except in the free-surface domain of the absorbing beach. Linear straight elements with linear variation of the flow variables over the elements were used. The collocation points were at the ends of the elements. A mixed Eulerian-Lagrangian method steps the solution forward in time by calculating the motion of the free-surface particles and the rate-of-change of their velocity potential. Body-free surface intersection was normally handled by requiring continuity of the velocity potential. If the angle between the free surface and the body is less than $\pi/30$–$\pi/20$, the free surface is cut at the intersection point. The experiments showed that the water always entered the deck in the form of a plunging breaker. The BEM was able to simulate that by enforcing a Kutta condition requiring the flow to leave tangentially the vertical bow side. Figure 7 shows a comparison between theory and experiments. Since surface tension matters in describing the details of the plunging wave in the model tests, this is included in the numerical simulations. An attempt was made by Greco *et al.* [36] to use the VOF method to simulate the plunging breaker. The results were less satisfactory than those obtained by the described BEM, although the feasibility of a domain-decomposition strategy, where only a limited portion of the computational domain is treated by a Navier-Stokes solver, was demonstrated.

When the plunging breaker hits the deck, very high pressures will occur. Since these pressure peaks are strongly concentrated in time and space, they are not expected to be important for the structure. A consequence of the impact, is that two jet flows are formed, moving respectively towards and away from the bow end. An air cavity is formed. As the air volume decreases, the air-cavity pressure is of concern for the structure. This is related to both the time duration and spatial extent of the pressure. Three-dimensional experiments for three different

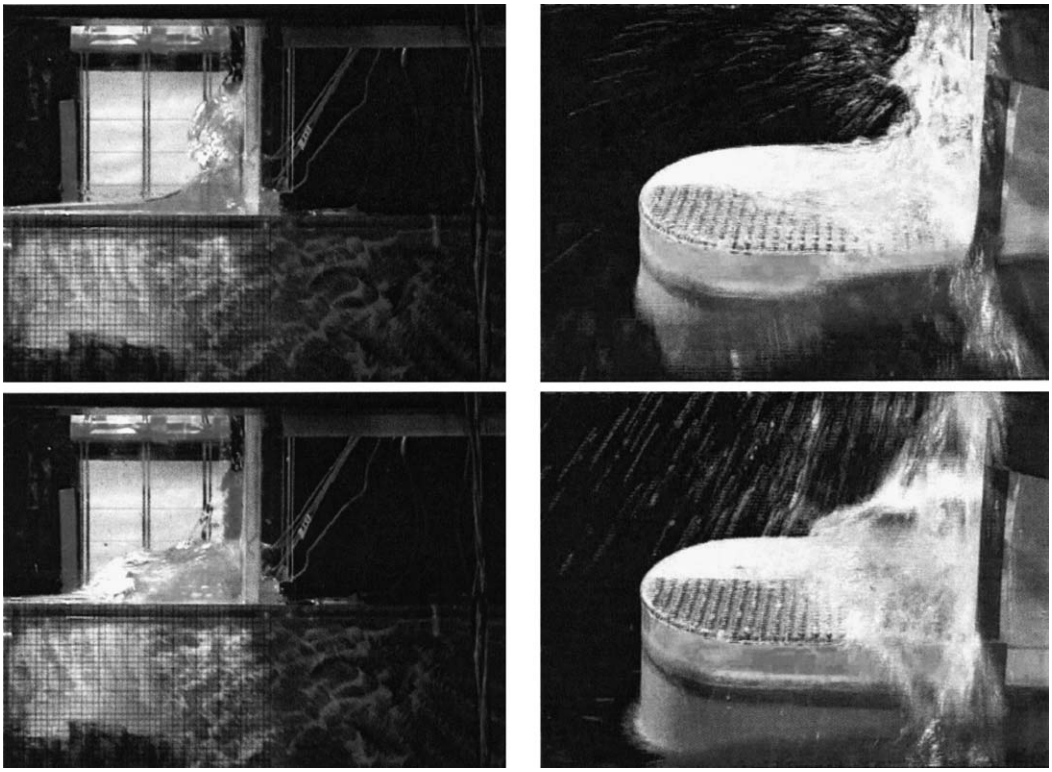

Figure 8. Late evolution of the impact against the vertical superstructure: backward plunging water front after the maximum run up. Left column: two-dimensional experiments, Greco [35]. Right column: three-dimensional model tests, Barcellona *et al.* [37].

bow forms of stationary ships restrained from moving were presented by Barcellona *et al.* [37]. They all show that the water enters the deck also in 3D always in terms of a plunging breaker and that an air cavity is formed. However, the experiments are not conclusive about air escape and development of high pressures due to the presence of an air cavity. The phenomenon with the plunging breaker does not seem to have been reported previously. One possible reason is that it may occur on a very small scale in space and time; other researchers have been more concerned about what happens later with the water on deck. Further, it is not so easily detected in three-dimensional tests. One must, of course, be careful when generalizing the results to any above-water hull form and to be valid for both zero and forward speeds. For instance, if the relative vertical velocity is very large with respect to the horizontal velocity, the overturning of the water during the water-shipping initiation may not happen at all. The reason is that the horizontal velocity plays an important role in the formation of the plunging breaker.

Returning now to the 2D situation, the air cavity will collapse into bubbles, which are convected with the fluid and end up on the free surface. The BEM is not able to model the collapse of the air cavity and for the subsequent numerical calculations it is required that both the deck and the vertical bow side are wetted at the bow end. This could, in principle, create a cross flow with vortex generation at the bow end of the deck. However, experimental flow visualizations do not indicate that. When the flow further develops along the deck, it has been popular to use a dam-break model. Since there is important communication between the flow on the deck and outside the deck, the numerical simulations showed that a dam-break model

does not provide a sufficiently accurate description. The BEM agrees well with experimental free-surface elevations as the water propagates along the deck. At a sufficient distance from the bow before hitting the vertical wall, the flow can be described by the shallow-water equations. Before the impact, the front end of the water is similar to a fluid wedge with an interior angle β, with practical values of the order of 40°, or less.

In [38] it is shown that, by neglecting gravity, the similarity solution by Zhang *et al.* [39] can be used to efficiently predict the initial slamming pressures. However, as water runs up along the vertical wall, gravity starts to matter and, in particular, the similarity solution becomes less and less accurate. The BEM agrees very well with experiments during this phase. When run-down of water starts, an overturning of the free surface develops and results in an impact with the underlying water. The experiments show that pressures of similar magnitude as in the initial impact phase occur on the vertical wall. The BEM breaks down during this last phase. By using the SPH method and a dam-break model, Colagrossi and Landrini [40] were able to also simulate the run-down phase along the vertical wall. Greco *et al.* [41] showed that local hydroelasticity is insignificant in evaluating maximum stresses due to impact on a deck house. This is a consequence of the duration of impact load relative to the highest natural period for local structural vibrations. A 2D flow situation, with a realistic amount of water and structural dimensions, was used. However, the resulting maximum stresses were significant. The 3D experiments by Barcellona *et al.* [37] measured the impact force on a vertical wall representing the front end of the deck house. These experiments indicate that impact pressures for 3D-flow situations are clearly largest during the initial impact phase. However, the run-down phase, where overturning impact on the underlying free surface causes significant pressures on the deck, should be of concern in design. The run-down phase appears even more complicated than in the 2D experiments and is accompanied by a substantial amount of spray. Figure 8 illustrates the run-down phase for 2D and 3D flow conditions.

The water flow on the deck of a FPSO in steep random waves with nonlinear effects were measured by a 10-staff wave array by Standsberg and Karlsen [42]. Some cases, resembling the dam-break-type flow, were the result of large negative bow motion with small initial horizontal fluid velocities (see the top drawing in Figure 1). Other observed cases did not show a typical dam-break-type behaviour and were more related to the kinematics of extreme (almost breaking) incident waves. These last circumstances caused highest impact loads on the deck house in the forepart of the FPSO. In particular, the experiments (*cf.* [42, Figure 2]) have shown the possibility that the water can hit the deck house directly without flowing along the deck first (as sketched in the center drawing of Figure 1). Numerical two-dimensional studies by Greco *et al.* [43] indicate that this requires the waves to be close to breaking ahead of the bow. A situation like this creates also the possibility of strong bow-stem slamming.

Finally, in the analyses reported above, the effects on water shipping of wave-induced motions and forward speed have not been considered. The traditional way to calculate the occurrence of water on the deck of a ship at forward speed is briefly summarized by Barcellona *et al.* [37]. The consequences on the deck flow and the possible related impact events against superstructures are open problems.

4.2. FUTURE CHALLENGES

The challenges associated with two-phase flow occurring during the initial impact of the water with the deck and during the run-down phase after impact against a vertical wall ought to be first considered in 2D-flow conditions. Tre Smoothed Particle Hydrodynamics (SPH) method

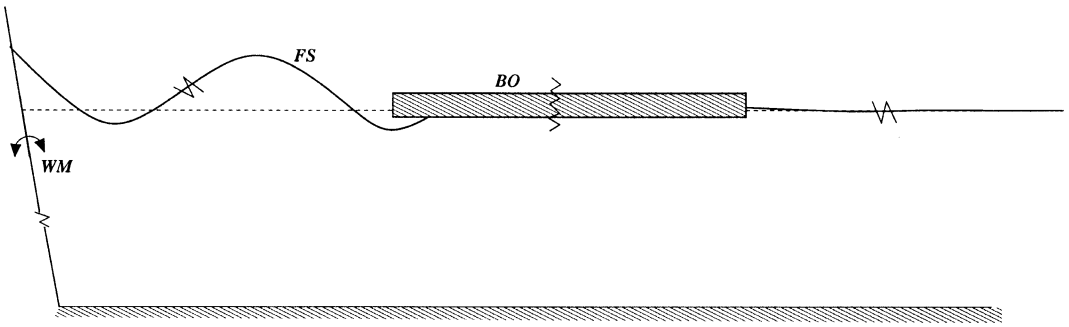

Figure 9. Analyzed two-dimensional problem.

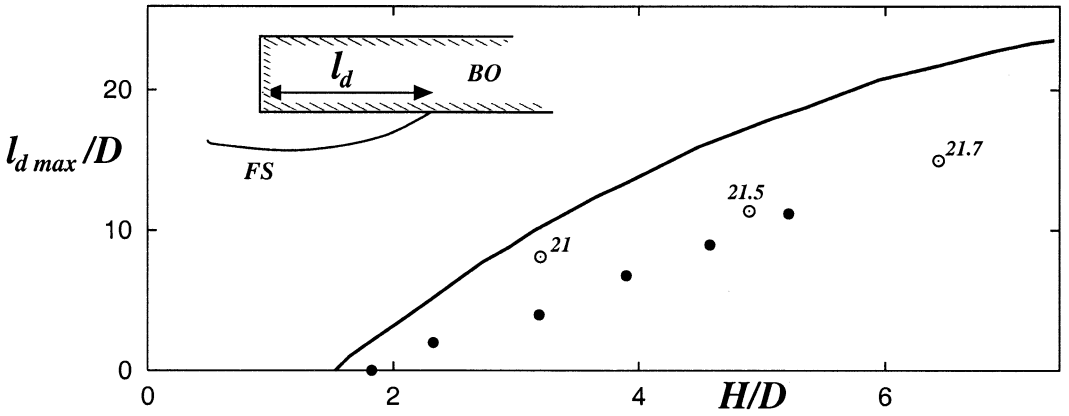

Figure 10. Maximum bottom emergence $l_{\mathrm{d\,max}}$ by two-dimensional experiments, •, and linear theory, solid line, by Yoshimoto *et al.* [45] for the highest-rigidity case (model B) and $T\sqrt{g/D} = 20{\cdot}06$. Our predictions for restrained model, °.

can handle such flows (see [40]). Since the method is very demanding from a CPU-point of view, it is more suitable for relatively limited fluid domains like the dam-break problem. A possibility is to use a Domain-Decomposition approach, where the SPH is used for the deck flow but a robust algorithm is needed to introduce or remove particles from the SPH domain due to the coupling with the outer-domain. In addition, it is not a simple task to analyze the nonlinear flow outside the deck of a ship. At a certain distance from the bow, the outer flow can probably be approximated by a second-order time-domain solution.

4.3. Green water and slamming on a VLFS with shallow draft

Wave-induced motions and loads on barge-type floating airports proposed in Japan have been extensively investigated by linear hydroelastic theory. Relevant airport dimensions are freeboard 5·5 m, draft 1·5 m, length 4770 m and breadth 2055 m. A representative water depth could be 20 m. There are limited studies on bottom slamming and green water. Since a survival condition could imply a significant wave height of 3·7 m and a significant wave period of 6·1 s, and diffraction matters, both bottom slamming and green water should be of concern. Concerning green-water occurrence, we are only aware of the experimental studies by Takaishi *et al.* [44]. Yoshimoto *et al.* [45] presented a two-dimensional experimental study on bottom slamming. Finally, Takagi [46] presented a theoretical approach to evaluate the

impact pressure during bottom slamming on a VLFS, and reported a convincing comparison with the experiments by Yoshimoto *et al.* [45].

Our numerical studies apply a two-dimensional numerical tank. BEM is used to solve the fully nonlinear potential-flow model without surface tension. The method has been experimentally validated for green-water loads on ship-like bodies [35]. The very shallow draft of a barge-type floating airport implies that bottom slamming will occur in wave conditions where water shipping on the deck happens. The flow conditions require the modelling of additional features which will be described in more detail later.

We model numerically a wavemaker generating regular waves incident on a barge-type VLFS with shallow draft and finite freeboard (see Figure 9) in transient and nearly steady-state conditions. The wave periods T and heights H are relevant to a floating airport. The length-to-draft ratio is $L/D = 120$ and the freeboard-to-draft ratio is $f/D = 3{\cdot}7$. The considered f/D is representative for a barge-type airport while a typical value for L/D would be of about 3000. Since in our case the body is restrained from moving, this difference in L/D is believed unimportant for studying details of the flow at the front edge. The wavemaker is located at $240D$ from the front edge of the body, about two to four wave lengths in the studied cases. The fluid depth is $60D$, which implies infinite fluid depth from a hydrodynamic point of view. A numerical wave beach is introduced starting at a distance $240D$ past the platform to limit the fluid domain and avoid unphysical wave reflection from the end of the computational domain. Since air cushions can be generated during bottom slamming, their effect on the water flow has been accounted for. This is done by neglecting the air flow and assuming the cavity pressure related to the cavity volume by an adiabatic relationship, *i.e.*

$$p = p_a \left[\frac{\mathrm{Vol}_0}{\mathrm{Vol}(t)} \right]^{\gamma}, \tag{1}$$

where p_a is the atmospheric pressure and Vol_0 is the initial volume at closure of the air cushion. By treating the air as an ideal gas, we used $\gamma = 1{\cdot}4$.

Once the draft is exceeded by the water, a portion of the VLFS bottom becomes dry, modifying relatively quickly the loading conditions on the structure. The maximum bottom emergence $l_{d\,\max}$ (defined in Figure 10) is a measure of the bottom area affected by slamming. In Figure 10, the experimental values of $l_{d\,\max}$ obtained by Yoshimoto *et al.* [45] for their model-B case are reported, $\bullet$, as a function of the incident wave height-to-draft ratio H/D, and are compared with the present numerical simulations, $^{\circ}$, for the indicated non-dimensional wave periods $T\sqrt{g/D}$. Here, g is the acceleration of gravity.

Actually, Yoshimoto *et al.* [45] considered two global rigidities. The model-B case corresponds to the highest rigidity, when the observed vertical motion amplitudes of the platform were the smallest and less than 15% of the incident wave amplitude.

For this case, the authors reported formation of air cushions during bottom slamming, similar to our numerical predictions. The theoretical result by Yoshimoto *et al.* [45] – solid line in Figure 10 – is based on linear hydroelastic theory and by assuming bottom-clearance occurrence when the amplitude of the dynamic pressure at a specific location is larger than the hydrostatic bottom pressure. These results for dynamic-pressure amplitude along the VLFS indicate that closed cavities, similar to those found by fully nonlinear simulations, cannot be predicted by their linear theory. Our prediction of maximum bottom emergence agrees better with the experiments than the linear theory does. However, the VLFS is moving in the experiments, while our model is restrained. This influences the results. For instance, the

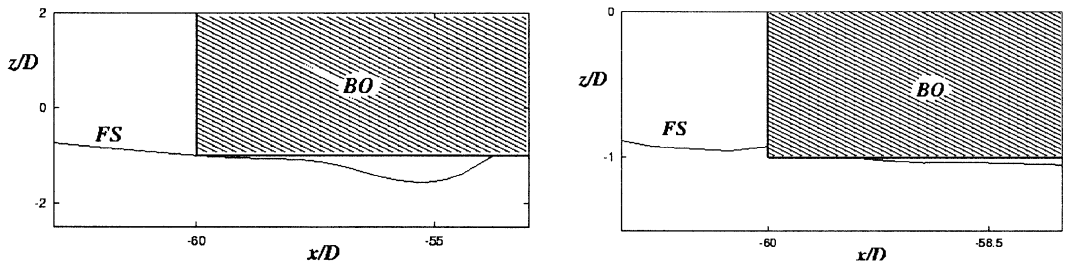

Figure 11. Left: Example of bottom impact. Right. Free-surface configuration by using a local-impact solution.

experiments by Yoshimoto *et al.* [45] on model A, with smaller global rigidity and larger vertical platform motions at the front end, showed that air cushions did not occur.

The left plot in Figure 11 shows a typical scenario during bottom slamming. The water hits the front edge of the body bottom. The angle between the free surface and the bottom is less than 4°, and very rapid changes of the wetted area next to the front edge occur.

In the following, a robust and reliable numerical treatment of this stage of the evolution is obtained by embedding a local analytical solution into the numerical procedure. To this purpose, we observe that, near the first impact location, the free surface can be approximated by a straight line. Second, we assume that the involved spatial and time scales are so small that the local solution can be seen as a perturbation of the flow variables numerically obtained at the impact instant. Finally, we neglect the possibility that, on the front side of the structure, air cavities of the type shown in water-shipping phenomena are formed.

A local analytical solution has been introduced and solved within the sub-domain $A \cup C$, defined in Figure 12. The analytical solution considers the impact of a flat free surface with an angle β between the free surface and the bottom surface. The initial impact position is the front edge. The water before the impact is assumed to have a constant vertical velocity V_0. The flow due to the impact can be solved as Wagner [2] did for two-dimensional impact of a rigid body on an initially calm free surface. The boundary-value problem is shown in Figure 12. The details of the jet flow at $x = 2c$ are not considered. An important difference with Wagner's analysis is that the body-free surface intersection point corresponding to the front edge of the bottom $x = 0$ does not change with time. In principle, a Kutta-like condition could be enforced there and this would be appropriate to model the initial stage of the entrapment of an air-cavity on the front side of the structure. Here, we rule out this phenomenon, and the fluid run-up along the front edge is handled by a local analysis in the sub-domain C, described later. The solution of the velocity potential φ on the wetted surface is

$$\varphi = -V_0\sqrt{x(2c - x)} \quad 0 < x < 2c(t). \tag{2}$$

The wetted length $2c(t)$ can be found by the kinematic free-surface condition. It results in an integral equation which is solved in the spirit of Wagner. The solution is $c = 2V_0t/(3\tan\beta)$, where $t = 0$ corresponds to initial impact time. The pressure on the wetted surface follows from $-\rho\partial\varphi/\partial t$. The free-surface elevation due to slamming is

$$\eta = V_0\int_0^t \frac{|x - c(t')|}{\sqrt{x(2c - x))}}\mathrm{d}t' - V_0t = \frac{1}{2}\tan\beta[(c - 2x)\sqrt{\frac{x - 2c}{x}} + 2x] - V_0t, \tag{3}$$

which is infinite at $x = 0$. This necessitates a more detailed analysis in the vicinity of the front edge where the instantaneous draft is accounted for. The barge appears as a semi-infinite

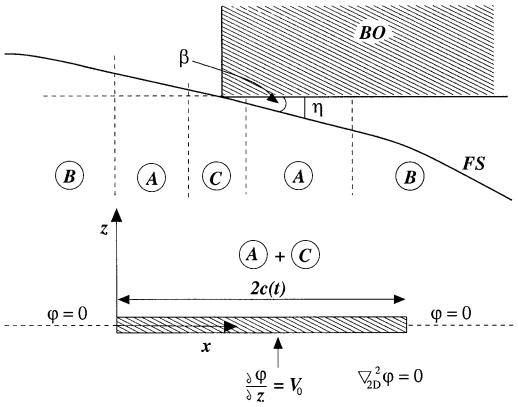

Figure 12. Top: Sub-domains A, B and C at bottom impact. Bottom: Boundary-value problem for φ due to bottom-slamming in sub-domains A and C. $x = 0$ front edge of bottom, $2c(t)$ = wetted length.

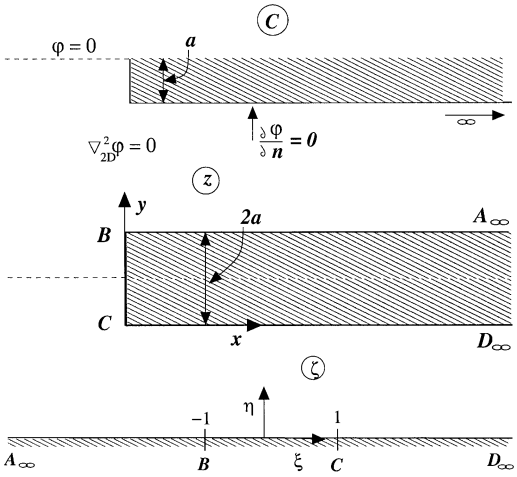

Figure 13. Local-flow analysis near front edge of VLFS bottom, sub-domain C. Top: boundary value problem. Center: body and image body. Bottom: Auxiliary ζ-plane in Schwarz-Christoffel transformation.

body in the analysis, *cf.* Figure 13, where $a(t)$ is the instantaneous draft to be determined by the analysis. The dynamic free-surface condition is $\varphi = 0$. The flow is solved by considering the body and its image, and a Schwarz-Christoffel transformation

$$z = \frac{2a}{\pi}[\zeta\sqrt{\zeta^2 - 1} - \log(\zeta + \sqrt{\zeta^2 - 1})], \tag{4}$$

to map the physical plane into the auxiliary ζ-plane, as shown in Figure 13. In (4), $z = x + \mathrm{i}y$ and $w = U\zeta$ is the complex potential. The complex velocity in the z-plane is

$$u - \mathrm{i}v = \frac{\mathrm{d}w}{\mathrm{d}z} = \frac{U\pi}{2a}\frac{1}{\sqrt{\zeta^2 - 1}}, \tag{5}$$

where U is determined by matching with the slamming solution. Equation (2) gives an inner expansion of the horizontal velocity near the front edge equal to $-V_0\sqrt{c/(2x)}$. The corresponding outer expansion of the inner solution is obtained by noting that Equation (4) gives $x \sim 2a\xi^2/\pi^2$ for large ξ ($\zeta = \xi + i\eta$). By using (5) we get the outer expansion $u = 0{\cdot}5U\sqrt{\pi/(2ax)}$ on the VLFS bottom. The matching gives $U = -2V_0\sqrt{ac/\pi}$. We will now determine $a = A_1 t$ by using the vertical velocity v at the body-free surface intersection point in the local front-edge solution, *i.e.*

$$a = \int_0^t v\mathrm{d}t' + V_0 t, \tag{6}$$

where $v = 0{\cdot}5\sqrt{\pi c/a}$. This gives that A_1 is determined by the cubic equation

$$A_1^3 - 2V_0A_1^2 + V_0A_1 - \frac{V_0^3\pi}{6\tan\beta} = 0, \tag{7}$$

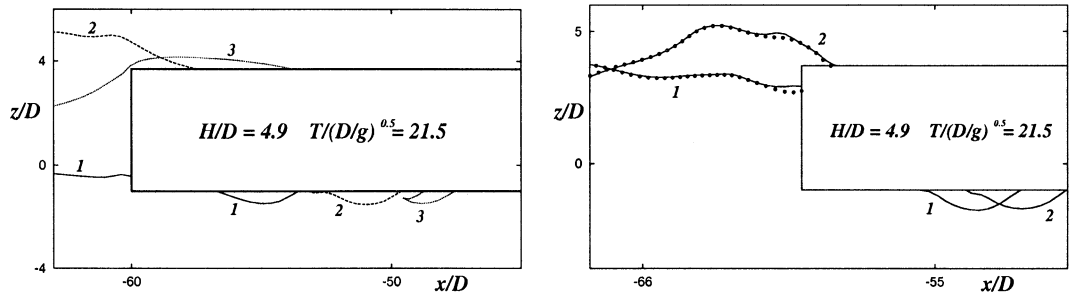

Figure 14. Left: Full-scale evolution of the cavity, $D = 1{\cdot}5$ m. Right: Free-surface evolution accounting, solid lines, and not accounting, •, for the cavity evolution. The free-surface configurations are enumerated as the time increases.

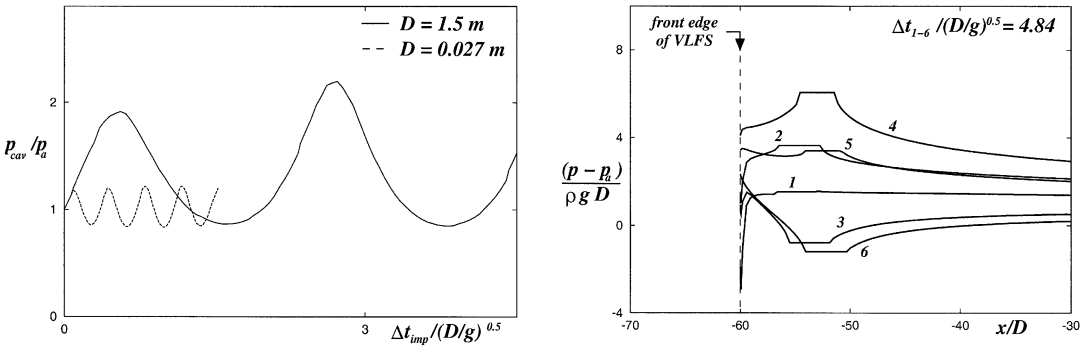

Figure 15. Left: Pressure evolution in the cavity in full scale ($D = 1{\cdot}5$ m, solid line) and in the scale of experiments ($D = 0{\cdot}027$ m, dashed line) by Yoshimoto *et al.* [45]. Right: Pressure evolution along the VLFS bottom in full scale. Δt_{1-6} = time difference between instants numbered 6 and 1.

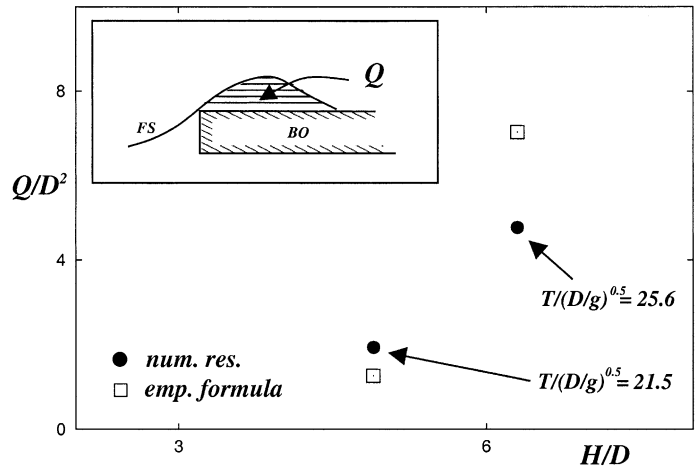

Figure 16. Comparison of the volume of the numerically shipped water with the empirical formula in [47].

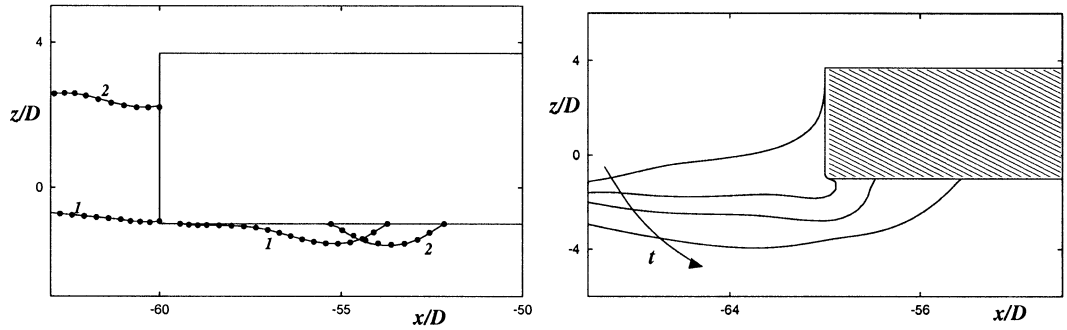

Figure 17. Left: Free-surface configurations after the bottom impact for body radius of curvature $R/D = 0{\cdot}01$, solid lines, and $R/D = 0{\cdot}2$, •, and same draft $D = 1{\cdot}5$ m. Free-surface profiles are enumerated as time increases. Right: Turning phenomenon for $R/D = 0{\cdot}2$, $D = 1{\cdot}5$ m.

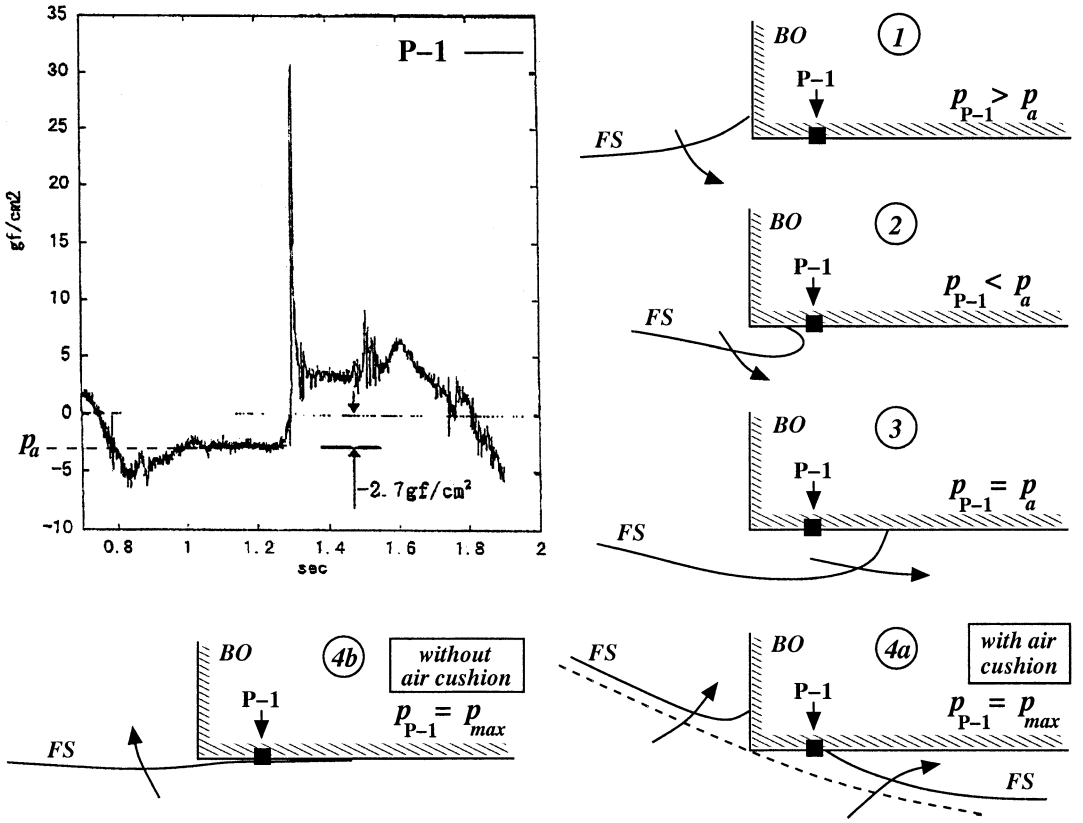

Figure 18. Pressure measurements by Yoshimoto *et al.* [45] at location P-1 ($D = 0{\cdot}027$ m) with Model A having smallest rigidity ($T = 1{\cdot}05$ s, $H = 13{\cdot}8$ cm). The numerical simulation (frames 1–4b) provides the physical interpretation of the experimental findings.

which has only one real root. The local analytical solution is incorporated in the BEM as follows. At the impact instant $t = 0$, the innermost sub-domains $A + C$ are characterized by an angle $\beta + \epsilon$ between the free surface and the body surface with $\epsilon < 1°$. The time duration t of the analytical slamming is determined through the given expression for c by deciding the maximum wetted length. Consistently, the free-surface elevation after time t is composed of two parts. One part, sub-domain B in Figure 12, uses the free-surface velocities at the initial time, and moves free-surface particles by an Euler time-stepping scheme. Since the analysis is only applied when β is very small, t will also be very small. This implies a small error, $\mathcal{O}(t^2)$, in using an Euler scheme. The other part, sub-domains A and C, is determined by (3), except at the free-surface intersection with the front-side walls (sub-domain C) where $a(t) = A_1 t$ is used. Equation (3) cannot be applied too close to this body-free surface intersection point. However, it turns out that a good patching can be obtained. We could have applied (5) to find the free-surface elevation in the portion of sub-domain A upstream of the front edge. It implies that a given x would correspond to different ζ as time changes. Since the flow due to slamming assumes the dynamic free-surface condition $\varphi = 0$, the change in φ at the free surface is determined by using the time rate of change of φ computed at the impact instant in combination with an Euler time-stepping scheme. On this short time scale, it is assumed that pressure variations due to volume changes in the nascent bottom air cavity are neglected.

The left plot of Figure 14 shows water evolution after the impact occurrence. The cavity deforms and moves under the influence of the surrounding flow. Finally it tends to detach from the structure and collapses. We cannot predict the collapse of the cavity into bubbles. This happens before a new water run-down with draft excess occurs. The cavity evolution affects the loads on the VLFS bottom but is unimportant for the flow evolution in front of the front-deck edge. This is confirmed by comparison with the free-surface evolution obtained by cutting the free-surface portion coinciding with the cavity surface after the bottom impact (see right plot of Figure 14). As we can see, except for a local area near the body, they are in satisfactory agreement. This means, if steady-state conditions are required, one can simply study the bottom impact occurring in such circumstances and cut the previous cavities.

The evolution of the cavity pressure relative to p_a during the first bottom impact is given in the top plot of Figure 15 for $H/D = 4{\cdot}9$ and $T\sqrt{g/D} = 21{\cdot}5$. The results refer to full scale ($D = 1{\cdot}5$ m) and experimental scale, $D = 0{\cdot}027$ m, used by Yoshimoto *et al.* [45]. In both cases an oscillating pressure is found, but the oscillation period reduces with the scale as well as the maximum pressure. The minimum pressure remains almost unchanged. From the results it appears that the cavity pressure does not scale with Froude number. If the experimental values were Froude-scaled, the experiments would predict larger cavity volumes more highly vibrating than in reality. Further, Froude scaling of $p - p_a$ from $D = 0{\cdot}027$ m to $D = 1{\cdot}5$ m gives about 9 times the value obtained numerically for $D = 1{\cdot}5$ m; *cf.* Figure 15. The bottom plot of Figure 15 shows the time evolution of the bottom pressure after the impact in the full-scale case. There is a large negative value of $p - p_a$ at the front edge at the first time instant shown, indicated as 1. This is associated with the quadratic velocity term in the Bernoulli equation and due to high cross-flow velocity at the edge. Since vortex shedding occurs in reality, we should be skeptical about the quantitative level of the negative $p - p_a$. The pressure is above cavitation pressure. The structural effect of the pressure loading will be discussed later.

The studies of water shipping on the deck do not include the previously described initial plunging breaker hitting the deck. The numerical amount of shipped water obtained for $H/D = 4{\cdot}9$, $T\sqrt{g/D} = 21{\cdot}5$ and for $H/D = 6{\cdot}3$, $T\sqrt{g/D} = 25{\cdot}6$ is presented in Figure 16

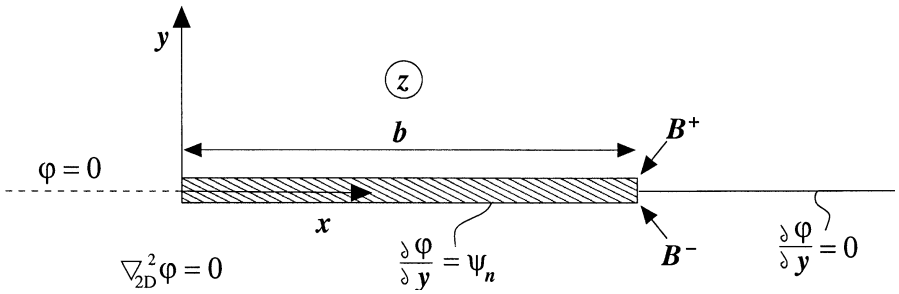

Figure 19. Sketch of the boundary-value problem associated with the forced oscillation with the mode shape ψ_n.

and compared with the empirical formula

$$Q = 2m\sqrt{2g}/3 \int_0^t [Z(t') - Z_0]^{3/2} \mathrm{d}t' \tag{8}$$

for estimating water volume of overtopping waves on a vertical breakwater [47]. The time refers to the starting of the water shipping and $[Z(t') - Z_0]$ represents the instantaneous freeboard excess by the water which is clearly influenced by nonlinearities. This has also been documented experimentally by Takaishi *et al.* [44]. As proposed by Kikkawa *et al.* [47], we set $m = 0{\cdot}5$. The numerical and experimental values are in reasonable agreement. However, since the mass flux of water through a vertical plane coinciding with the front side of the platform determines the water volume on the deck, the wave period must be an important parameter in addition to the wave amplitude. Takaishi *et al.* [44] compared all their experimental results for regular and irregular waves with different periods against the empirical formula with $m = 0{\cdot}7$. A large scatter occurred documenting that the approach is not sufficient for quantitative predictions.

After the run-down phase of the water along the front side, the free surface will turn rapidly around the front edge. This is associated with vortex separation from the sharp edge. However, the latter effect is neglected in our analysis. In order to facilitate the numerical simulations, the front edge has been rounded with a radius $R = 0{\cdot}2D$. This is relatively large in the scale of the local impact; however, the comparison between the free-surface evolution after the bottom impact with $R = 0{\cdot}2D$ and the smaller value $R = 0{\cdot}01D$ did not show substantial differences *(cf.* left plot of Figure 17).

Two main types of bottom turning have been observed. In the former, the local free surface near the front deck edge is relatively flat. This occurs during the transient and when the wave-body interaction is not characterized by large nonlinearities. In the latter, the local free surface running down the structure detaches from the body as a thin layer of fluid with a small angle between free surface and structure. The right plot of Figure 17 illustrates the free-surface configurations at different time instants during the second type of run-down. The free surface has a very small radius of curvature just after it has turned around the front edge of the bottom. We do not have experimental evidence for this for a VLFS. However, Baarholm [31] presented two-dimensional experimental results for wetdeck slamming that showed a similar behaviour (see Figure 5).

The turning of the free surface around the front edge during run-down is associated with the occurrence of local negative pressures $p - p_a$ due to high flow velocities, similar to the turning associated with the water run-up after the bottom impact. Other phases of the flow evolution are also connected with negative $p - p_a$. These have been indicated by the

experiments of Yoshimoto *et al.* [45] as shown in the top left plot of Figure 18, showing the pressure time evolution at the location P-1 at about 1·48*D* from the front edge. Here $p = -2{\cdot}7$ gf/cm^2 (265 Pa) corresponds to the atmospheric pressure p_a since the hydrostatic value has been subtracted from the pressure record. As we can observe, at the beginning of the shown time evolution, the pressure reduces, attains negative values for about 0·2 s, then it increases, becoming atmospheric for about 0·3 s and after that the maximum value is reached. These stages can be explained through the sketches 1–4 in the same figure. Before the bottom turning of the water, the pressure exceeds p_a (sketch 1). After the turning, the free surface is locally characterized by high curvature and propagates along the bottom approaching location P-1. This 'water-exit' phase is associated with negative pressures mainly due to the positive values of $\partial\varphi/\partial t$ (sketch 2). Yoshimoto *et al.* speculated that the negative pressures were due to surface tension. It is true that surface tension may affect flows with high curvature of the free surface. However, the main effect is due to fluid-acceleration expressed in terms of $\partial\varphi/\partial t$. Once the water front leaves P-1, this location remains dry, the pressure becoming atmospheric (sketch 3). This lasts until the bottom impact occurs affecting the considered location, so that $p = p_{\max}$. This can be associated with air-cushion formation and thus start from the front edge (sketch 4a) or can occur without air entrapment, starting from the maximum distance of the bottom-free surface intersection from the front edge (sketch 4b). The latter occurred during the shown experimental case.

The structural effects of the bottom-impact loading, as presented in Figure 15, will be assessed by hydroelastic analysis (see *e.g.* [15]). The stiffened bottom plating with longitudinal stiffeners between two transverse stiffeners is modeled by an equivalent beam. Only the equivalent beam next to the front edge is considered. The following hydrodynamic simplifications are made. The excitation pressure assumes a rigid body. The pressure due to the beam oscillations is estimated by neglecting the air cushion.

The beam equation is solved by expressing the beam deformations as $w = \Sigma a_n(t)\psi_n$, where ψ_n are dry normal modes and $a_n(t)$ are generalized coordinates. The flow due to forced oscillation of the beam with velocity ψ_n is found by solving the boundary-value problem in Figure 19. The problem is solved by the conformal mapping $z = b\zeta^2$, where $z = x + \mathrm{i}y$, and the physical plane corresponds to $y < 0$. The lower B^- and upper B^+ points of the vibrating beam of length b correspond to $(\xi, \eta) \equiv (-1{,}0)$ and $(\xi, \eta) \equiv (+1{,}0)$, respectively, in the auxiliary plane $\zeta = \xi + \mathrm{i}\eta$. The problem in the ζ-plane can be solved by a source distribution between $\xi = -1$ and 1 for $\eta = 0$. The source strength is determined analytically by the body boundary condition. If the beam equation is multiplied by ψ_m and integrated over the beam length, the pressure due to ψ_n determines generalized added-mass terms A_{mn} appearing in the resulting equation system. The expressions are

$$A_{mn} = \rho\frac{4b^2}{\pi}\int_0^1 u\psi_n[x(u)]\mathrm{d}u\int_{-1}^1 \xi^\star \log|u + \xi^\star|\psi_n[x(\xi^\star)]\mathrm{d}\xi^\star, \tag{9}$$

where $x(u) = bu^2$ and $x(\xi^\star) = b\xi^{\star 2}$. This means the equation of motions of the generalized coordinates are

$$(M_{mn} + A_{mn})\ddot{a}_n + M_{mn}\omega_n^2 a_n = \bar{p}_m \tag{10}$$

with

$$\bar{p}_m = \int_0^b p_e(x)\psi_m \mathrm{d}x \tag{11}$$

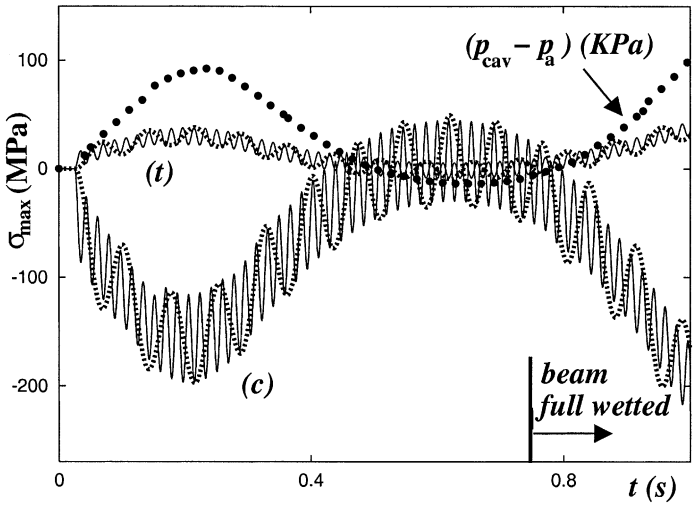

Figure 20. Full-scale maximum tension (t) and compression (c) stresses on the beam during the first bottom impact for $H/D = 4{\cdot}9$ and $T\sqrt{g/D} = 21{\cdot}5$. Solid lines: dry-mode response. Dashed lines: approximate hydroelastic response. •: cavity pressure. $t = 0$ s is the impact time. For $t \geq 0{\cdot}75$ s the beam is fully wetted.

and

$$M_{mn} = \int_0^b m\psi_m\psi_n \mathrm{d}x. \tag{12}$$

Here m is the structural mass per unit length and unit width of the beam and ω_n is the n-th dry natural frequency which is equal to $\lambda_n^2\sqrt{EI/m}$, where EI is the beam bending stiffness and λ_n is the n-th eigenvalue. Taking into account the effect of air cushion on the added mass would require a numerical solution. This is not pursued further. Our objective is to qualitatively judge the importance of hydroelasticity.

The case study considers structural mass per unit length and breadth $240{\cdot}7$ Kg/m^2, beam bending stiffness $EI \simeq 27{\cdot}5$ MNm^2 and a distance from the neutral axis to where maximum stresses occur $z_a \simeq 0{\cdot}23$ m. The beam has a length $b = 5$ m and it is clamped at the ends.

The time evolution of maximum tension and compression stresses at the end position is shown in Figure 20 together with the pressure inside the cavity. For $t \geq 0{\cdot}75$ s the beam is fully wetted. Results are given both for a dry-mode solution, solid lines, and for the previously described approximate hydroelastic theory, dashed lines. On a large time scale, the stress evolution follows the cavity pressure in a quasi-steady manner. The high-frequency oscillations are related to first-mode vibrations, with lower frequency in case of the approximate hydroelastic theory (dry natural period $\sim 0{\cdot}018$ s, approximate wet natural period $\sim 0{\cdot}073$ s). In this case study, the hydroelastic effects are not dominant. The maximum absolute value of the stress is $\sim$200 MPa and it should for instance be related to yield stress 320–360 MPa for high strength steel (NK standard).

5. Sloshing and slamming

5.1. STATUS

Sloshing is a violent resonant free-surface flow with strong nonlinear behaviour in a partially filled tank. Slamming is an important design load. A proper estimate of slamming is strongly connected with the global flow in the tank. The main interest is in excitation with frequency content in the vicinity of the highest natural period of the fluid motion. The corresponding linear mode of the motion for a rectangular tank with two-dimensional flow is an antisymmetric standing wave with wavelength twice the tank length.

It has become popular to use Computational Fluid Dynamics (CFD) to model sloshing. The problem has to be solved in the time domain due to the strong nonlinearities associated with the free surface conditions. There exists a broad variety of numerical methods. The Load committee of the 13th ISSC has provided a survey in 1997. Normally Reynolds-averaged Navier-Stokes Equations (RANSE) are solved, but also Euler equations or potential flows for incompressible fluid are used. 2D flow studies are most common. Finite Difference Methods (FDM), Finite Volume Methods (FVM) or Finite Element Methods (FEM) numerically solve the field equations. The use of BEM is based on a velocity potential satisfying Laplace equation. Methods based on field discretization can handle nonlinear free-surface motion by height-function method, marker method, Volume of Fluid (VOF) method, or a Level-Set method. More recently, mesh-less methods have been developed to deal with large deformations and even fragmentation of the free surface. Among these, Smoothed Particle Hydrodynamics (SPH), Monaghan [48], is currently under testing for sloshing problems [49]. Results are presented in Figure 21. Good agreement with BEM solutions up to breaking has been obtained. Long-time simulation for cases with large excitation amplitudes shows the ability to follow the post breaking behaviour. BEM breaks down after wave breaking occurs, while SPH is robust.

What then are the advantages and the disadvantages of using CFD? Advantages are that complex tank geometry, any fluid depth and general excitation may, in principle, be considered. A CFD method may provide good flow visualization, which is helpful in understanding the flow physics. Flow separation around internal structures can be simulated by a RANSE code. A disadvantage is that the CFD method is very time-consuming, which makes statistical estimates of tank response variables in a representative set of design sea conditions difficult. Some methods may not be robust enough. For instance, a mixed Eulerian-Lagrangian approach based on BEM breaks down when an overturning wave hits the free surface. Numerical problems may also arise with BEM at the intersection between the free surface and the tank boundary. Landrini *et al.* [50] discussed numerical problems associated with BEM and sloshing. If not sufficient care is exercised, some of the methods may degenerate numerically or generate fluid mass on a long time scale. Since the highest natural period is strongly dependent on fluid mass and fluid behaviour is strongly dependent on the natural period, this can result in an unphysical numerical simulation. This was demonstrated by Solaas [51] by using the commercial multipurpose FLOW-3D code, developed by Flow Science Inc. The method uses a combination of the SOLA finite-difference scheme for solving the Navier-Stokes equations and the VOF technique for capturing the free boundaries of the fluid. Kim [52] has presented a CFD method where conservation of fluid mass is satisfied. The amount of fluid in the tank is corrected for each time step by slightly moving the free surface. The correction is so small that the global motion is not affected. There exist examples on satisfactory predictions of non-

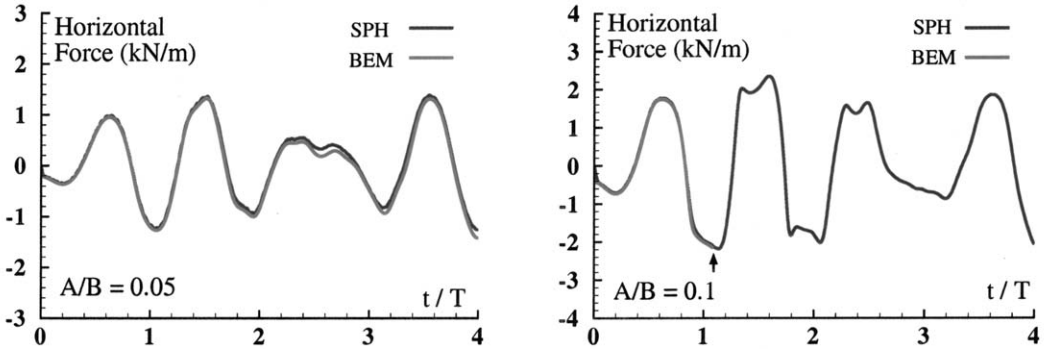

Figure 21. SPH simulation of 2D sloshing flow in rectangular tank without roof. Breadth $B = 1{\cdot}38$ m, fluid depth is $h = 0{\cdot}552B$, the highest natural period is $T_n = 1{\cdot}44$ s. The tank is forced to sway as $A \sin 2\pi t/T$, with period $T = 2$ s. Top diagrams: the horizontal force is compared with BEM computations by Landrini *et al.* [50]. For the largest sway amplitude (right plot), surface breaking prevents BEM computations to continue at time instant marked by the vertical arrow.

impacting loading by CFD *e.g.* [51], [53]). The Load committee of the *13th* ISSC presented a comparative study by 12 different CFD codes belonging to different classification societies, a shipyard, research organizations and universities. The agreement in predicting free surface elevations was not convincing, even in non-extreme cases.

It seems generally accepted that CFD codes have difficulties in predicting impact loads. This was also the conclusion of the Load committee of the 13th ISSC in 1997. Difficulties occur in particular when rapid changes in time and space happen. Few codes include hydroelasticity during impact. However, when doing so, the structural modelling requires also special care. Many structural modes are initially excited, when hydroelasticity is important. This, in combination with rapid changes of wetted surface influenced by the body vibrations, can easily cause numerical problems [54].

An alternative to CFD is to use more analytically oriented methods. An example of this are the studies by Faltinsen *et al.* [55], Faltinsen and Timokha [56, 57) for 2D flow in rectangular or nearly rectangular tanks and by Faltinsen *et al.* [58] for a square-based tank. The procedure is based on a Bateman-Luke variational principle and use of the pressure in the Lagrangian of the Hamilton principle. This results in a system of nonlinear ordinary differential equations in time. The unknowns are generalized coordinates β_i of the free-surface elevation. The method is robust and very time-efficient. Extensive validation was documented by comparing with model tests. The Fourier representation of the free surface implies that there are no overturning waves, vertical tank sides in the free surface, no effect of the tank roof and that the free surface intersects the tank wall perpendicularly. The latter means that run-up along the walls in terms of a thin sheet of water is poorly described. Run-up is a typical phenomenon for resonant sloshing in intermediate and shallow depths. If we refer to 2D flow in a tank with depth h and breadth B, then shallow depth means $h/B < 0{\cdot}1$ and intermediate depth $0{\cdot}1 < h/B < 0{\cdot}24$. The method assumes an incompressible fluid in irrotational motion. This is an appropriate approximation for finite depth and a smooth tank. However, when the fluid depth decreases from finite to intermediate and shallow depths, there is an increased importance of dissipation. This may for instance happen due to run-up along the tank wall and subsequent overturning of the free surface. Breaking waves in the middle of the tank may also occur for intermediate depth. The method is based on asymptotic relations where the tank motion is assumed small

and of $\mathcal{O}(\epsilon)$. Since the fluid motion is amplified at resonance, the fluid motion is assumed to be of smaller order than ϵ. This is done by relating the generalized coordinates β_i, for the free-surface elevation to different natural modes of fluid motion and deciding which modes are dominant. This is a function of secondary resonance, which means that higher natural modes are excited due to nonlinear fluid effects. This happens if natural frequencies are close to being multiples of the main resonance frequency. In the extreme case of shallow-fluid potential flow, all the natural frequencies are multiples of the lowest one. However, in practice, only a finite number of eigenmodes plays a role due to viscosity. An adaptive multi-modal approach where several modes may be dominant has been examined for 2D flow. When the fluid depth is finite, the generalized coordinates β_i, associated with primary modes are assumed $\mathcal{O}(\epsilon^{1/3})$. More than one primary mode matters near the critical fluid depth of $h/B = 0{\cdot}337$. Further, the higher the tank excitation amplitude is, the more important it will be to consider more than one dominant mode. As the fluid depth decreases and the intermediate and shallow depth range is reached, secondary resonance of higher modes is easily triggered. Both β_i associated with primary modes and h/B are assumed $\mathcal{O}(\epsilon^{1/4})$. Traveling waves are features of the flow at intermediate and shallow depth. When the excitation amplitude is sufficiently high, hydraulic jumps are formed at shallow depth. Many modes are needed to describe this phenomenon.

Roof impact is more likely to occur during realistic sloshing in ship tanks. This has been handled for finite fluid depth and a horizontal or chamfered tank roof by using a multi-modal approach for the ambient flow and account for the effect of impacts by the inclusion of linear damping terms in the equation system. The level of damping is such that energy drawn from the ambient flow is equal to the energy dissipated as a consequence of the impacts. The kinetic and potential energy is assumed lost in the impacts as the fluid falls down as 'rain' on the underlying free surface. The flow due to roof impact is modelled by a Wagner approach. The impacting free surface is assumed to have a parabolic shape with an impacting velocity varying linearly with time. The energy in the jet flow is calculated. It consists of kinetic and potential energy, which is assumed, dissipated during the subsequent impact with the free surface [59]. The method assumes that a standing-wave type of resonant fluid motion occurs, which means that it is appropriate for finite depth. A rigid tank was assumed in the analysis. However, hydroelasticity may be important. Faltinsen [60] studied tank-roof impact for finite depth by assuming the tank roof to be rigid and allowing for hydroelastic vibrations in the tank wall adjacent to the tank wall. The assumptions were otherwise the same as in [59]. Realistic dimensions for a ship tank made of steel were used and it was demonstrated that hydroelasticity matters for maximum stresses in the structure.

5.2. Future challenges

Even if progress has been made both by using CFD and by analytically oriented methods to describe sloshing in ship tanks, there are no tools that can handle any flow situation in a general tank shape. This is true even without slamming happening. The majority of studies are related to 2D flow, but important 3D flow effects may matter in reality. This was demonstrated by Faltinsen *et al.* [58] both theoretically and experimentally for a square based tank. Stability of steady-state solutions was examined. Swirling (rotational wave motion) may occur. For certain frequency ranges a steady-state motion may not exist. Instead a chaotic motion occurs. This is an important guidance for CFD developments. One may easily think that chaotic motions may be due to numerical approximations when computational methods are applied. The analysis assumed finite depth and used a multimodal approach as previously described for 2D

flows. This needs to be further developed for intermediate and shallow depths, as well as for situations where tank-length-to-breadth ratio is not equal to unity. Since dissipation matters for intermediate and shallow depths in a smooth tank, the previously described analytically oriented method should be further developed to deal with this effect. It would require studies of local solution that more properly model the run-up. This may be done analytically. A difficulty is how to couple that with the previously described modal method. Another matter is the run-down associated with the overturning of the free surface and subsequent impact on the underlying flow. It is hard to imagine that this local flow can be modelled analytically. A possibility is to use simulations by the analytically oriented method as an initial condition for a CFD calculations. Later on an analytically oriented method can be switched on by means of initial conditions from CFD.

There are several slamming scenarios that need more attention. One example is a shallow-fluid condition when a hydraulic jump is traveling back and forth in the tank. An air cushion may be generated during the impact. This impact situation has similarities with the hydroelastic drop tests described in section 2. It implies that one should focus on maximum stresses in the structure instead of pressure for a tank made by steel. As already stated, the pressure could be very high and highly localized in time and space, as well as being sensitive to inflow conditions.

Slamming loads on possible internal structures must also be considered. Some internal structures, like a horizontal stringer on the wall or web-frame at the tank roof, may be in and out of the fluid so that impact loads as well as non-impulsive loads may play a role.

Other complicated flow phenomena can occur. The impact on the tank roof can be so strong that the resulting jet flow shoots across the tank and hits the opposite wall. Further, fluid and gas will mix for heavy sloshing with wave breaking and boiling occurring in LNG tanks. This means that two-phase flow and the effect of ullage pressure, *i.e.* pressure on the free surface, should be considered. Since gas content in a fluid-like water or LNG can significantly lower the sound velocity, compressibility will last longer during impact and may therefore be more important from a structural point of view.

How slamming affects membrane tanks on LNG carriers need further attention. Two layers of membranes and insulation cover the tank walls. The insulation consists of foam and may be strengthened by plywood. How this structure reacts dynamically to slamming has to be understood.

The significance of the many different physical effects for slamming-induced structural stresses is also important for knowing how to scale model-test results.

6. Conclusions

Status and future challenges for water entry on an initially calm free surface, wet deck slamming, green water and sloshing have been presented. An important message is that slamming should be considered in the framework of structural-dynamics response. This implies that physical effects may be disregarded and very high pressures concentrated in time and space may not matter. Since slamming can be sensitive to the ambient flow, slamming analysis should ideally be integrated with the global-flow analysis around a ship or ocean structure or with the violent fluid motion inside a tank. However, even if slamming is disregarded, there are several remaining difficulties in describing violent fluid motions theoretically. Two-phase flow can be of practical importance for slamming and needs to be better understood.

Green water and slamming on a VLFS with shallow draft have been treated in more detail. A two-dimensional numerical wave tank based on BEM for fully nonlinear free-surface potential flow is applied to green water and bottom slamming on a restrained barge type floating airport with shallow draft. Since the angle between the impacting free surface and the bottom can be very small, a local analytical solution has been included in the numerical solver. The rapid turn of a highly curved free surface around the front bottom edge requires also special attention. Air cavities are found both during bottom slamming and in the initial phase of water entering the deck. This causes important loading and implies that experimental pressures cannot be Froude-scaled.

References

1. T. Von Kármán, The impact of seaplane floats during landing. *Nat. Adv. Com. for Aeronautics*. Tech. Note 321 (1929) 309–313.
2. H. Wagner, Über Stoss- und Gleitvorgange an der Oberfläche von Flüssigkeiten. *ZAMM* 12 (1932) 192–235.
3. R. Cointe and J. L. Armand, Hydrodynamic impact analysis of a cylinder. *J. Off. Mech. Arctic Engng.* ASME 109 (1987) 237–243.
4. R. Cointe, Free-surface flows close to a surface-piercing body. In: T. Miloh (ed.), *J. Mathematical Approaches in Hydrodynamics*. Philadelphia: SIAM (1991) 319–334.
5. Z. N. Dobrovolskaya, On some problems of similarity flow of fluid with a free surface. *J. Fluid Mech.* 36 (1969) 805–829.
6. R. Zhao and O. M. Faltinsen, Water entry of two-dimensional bodies. *J. Fluid Mech.* 246 (1993) 593–612.
7. R. Zhao, O. M. Faltinsen and J. Aarnes, Water entry of arbitrary two-dimensional sections with and without flow separation. In: *Proc. of 21st Symp. on Naval Hydrod.* Trondheim: National Academy Press (1997) pp. 408–423.
8. O. M. Faltinsen, Water entry of a wedge with finite dead rise angle. *J. Ship Res.* 46 (2002) 39–51.
9. A. A. Korobkin, Blunt-body impact on a compressible liquid surface. *J. Fluid Mech.* 244 (1992) 431–453.
10. A. A. Korobkin, Blunt-body impact on the free surface of a compressible liquid. *J. Fluid Mech.* 263 (1994) 319–342.
11. A. A. Korobkin, Acoustic approximation in the slamming problem. *J. Fluid Mech.* 318 (1996), 165–188.
12. A. A. Korobkin, Water impact problems in ship hydrodynamics, In: M. Ohkusu (ed.), *Advances in Marine Hydrodynamics.* Southampton: Computational Mechanics Publication (1996) pp. 323–371.
13. A. A. Korobkin, *Compressible Liquid Impact*. Novosibirsk: Siberian Branch of the Russian Academy (1997) 200 pp. (in Russian).
14. J. H. G. Verhagen, The impact of a flat plate on a water surface. *J. Ship Res.* 11/4 (1967) 211–223.
15. O. M. Faltinsen, Hydroelastic slamming. *J. Mar. Sci. Technol.* 5/2 (2000) 48–65.
16. A. A. Korobkin and T. I. Khabakhpasheva, Periodic wave impact onto an elastic plate. In: J. Piquet (ed.), *Proc. 7th Numerical Ship Hydrodynamics*. Nantes (1999) 7.3 pp. 1–19.
17. O. M. Faltinsen, Water entry of a wedge by hydroelastic orthotropic plate theory. *J. Ship Res.* 43 (1999) 180–193.
18. J. Kvaalsvold and O. M. Faltinsen, Hydroelastic modelling of wet deck slamming on multihull vessels. *J. Ship Res.* 39/3 (1995) 225–239.
19. O. M. Faltinsen, The effect of hydroelasticity on slamming. *Phil. Trans. R. Soc. London* A355 (1997) 575–591.
20. E.M. Haugen, *Hydroelastic Analysis of Slamming on Stiffened Plates with Application to Catamaran Wetdeck.* Ph.D. Thesis. Trondheim: Dept. Marine Hydrodynamics NTNU (1999) 170 pp.
21. R. Zhao, O. M. Faltinsen and H. Haslum, A simplified nonlinear analysis of a high speed planing craft in calm water. In: *Proc. of FAST'97*. Sydney 1 (1998) 431–438.
22. N. de Divitiis and L. M. de Socio, Impact of floats on water. *J. Fluid Mech.* 471 (2001) 365–379.
23. L. Sedov, *On the Theory of Unsteady Planing and the Motion of a Wing with Vortex Separation.* NACA Technical Memorandum 942 (1940) 53 pp.
24. T. Ulstein and O. M. Faltinsen, Two-dimensional unsteady planing. *J. Ship Res.* 40/3 (1996) 200–210.
25. T. Miloh, Wave slam on a sphere penetrating a free surface. *J. Engng. Math.* 15 (1981) 221–240.

26. O. M. Faltinsen and R. Zhao, Water entry of ship sections and axisymmetric bodies. In: *High Speed Body Motion in Water*. AGARD Report 827 (1998) 21-1-24-11.
27. Y. M. Scolan and A. A. Korobkin, Three-dimensional theory of water impact. Part 1. Inverse Wagner problem. *J. Fluid Mech.* 440 (2001) 293–326.
28. R. Zhao and O. M. Faltinsen, Water entry of arbitrary axisymmetric bodies with and without flow separation. In: *Proc. 22nd Symp. on Naval Hydrod*. Washington D.C.: National Academy Press, Washington D.C. (1998) pp. 652–664.
29. T. Ulstein, *Nonlinear Effects of a Flexible Stern Seal Bag on Cobblestone Oscillations of an SES*. Ph.D. Thesis. Trondheim: Dept. Marine Hydrodynamics NTNU (1995) 220 pp.
30. M. Landrini, A. Colagrossi and M. P. Tulin, Numerical studies of wave breaking compared to experimental observations. In: *Proc. of Fourth Numerical Towing Tank Symposium*. Hamburg (2001) 5 pp.
31. R. J. Baarholm, *Theoretical and Experimental Studies of Wave Impact Underneath Decks of Offshore Platforms*. Ph.D. Thesis. Trondheim: Dept. Marine Hydrodynamics NTNU (2001) 161 pp.
32. C. Ge, *Global Hydroelastic Response of Catamarans due to Wetdeck Slamming*. Ph. D. Thesis. Trondheim: Dept. Marine Technology NTNU (2002) 189 pp.
33. N. Salvesen, E. O. Tuck and O. M. Faltinsen, Ship motions and sea loads. *Trans. Soc. Nav. Arch. and Mar. Eng.* 78/10 (1970) 250–287.
34. O. D. Okland, *Theoretical and Experimental Analysis of Wetdeck Slamming*. Ph.D. Thesis. Trondheim: Dept. Marine Technology NTNU (2002) 206 pp.
35. M. Greco, *A Two-Dimensional Study of Green- Water Loading*. Ph.D. Thesis. Trondheim: Dept. Marine Hydrodynamics NTNU (2001) 150 pp.
36. M. Greco, O. M. Faltinsen and M. Landrini, Water shipping on a vessel in head waves. In: *Proc. of 24th Symp. on Naval Hydrodynamics*. Fukuoka (2002) 2.40–52.
37. M. Barcellona, M. Landrini, M. Greco and O. M. Faltinsen, An experimental investigation on bow water shipping. J. Ship Res. Vol. 47, No. 4, 2003.
38. O. M. Faltinsen, M. Greco and M. Landrini, Green water loading on a FPSO. JOMAE 124(2): 97–103, 2002.
39. S. Zhang, D. K. P. Yue and K. Tanizawa, Simulation of plunging wave impact on a vertical wall. *J. Fluid Mech.* 327 (1996) 221–254.
40. A. Colagrossi and M. Landrini, Numerical simulation of 2-phase flows by smoothed particle hydrodynamics. In: *5th Numerical Towing Tank Symposium.* Pornichet (2002) 6 pp.
41. M. Greco, O. M. Faltinsen and M. Landrini, Impact flows and loads on ship-deck structures. To be published in *J. Fluids Struct.* 2004.
42. C. T. Standsberg, S. Karlsen (2001), Green sea and water impact on FPSO in steep random waves. In: *Proc. PRADS'2001*. Shanghai 1 (2001) pp. 593–601.
43. M. Greco, O. M. Faltinsen and M. Landrini, Basic studies on water on deck. In: *Proc. of 23rd Symp. on Naval Hydrodynamics.* Val de Reuil: National Academy Press (2000) pp. 108–123.
44. Y. Takaishi, K. Minemura and K. Masuda, Experimental study on relative motion and shipping water of mega-float structure. *OMAE98-4995* Lisbon (1998) 8 pp.
45. H. Yoshimoto, K. Ohmatsu, S. Ohmatsuandi and T. Ikebuchi, Slamming load on a very large floating structure with shallow draft. *J. Mar. Sci. Technol.* 2 (1997) 163–172.
46. K. Takagi, A theoretical approach to the slamming impact pressure acting on the VLFS. *Int. J. Off. Polar Engng.* 12 (2002) 9–15.
47. H. Kikkawa, H. Shiagai and T. Kono, Fundamental study on wave overtopping sea dikes. In: *Proc. Coastal Engineering*. JSCE (1967) pp. 118–122.
48. J. J. Monaghan, Smoothed particle hydrodynamics. *Ann. Review Astron. Astrophys.* 30 (1992) 543–574.
49. M. Landrini, A. Colagrossi and O. M. Faltinsen, Sloshing in 2-D flows by the SPH method. *Proc. 8th International Conference on Numerical Ship Hydrodynamics*, Korea (2003).
50. M. Landrini, G. Grytoyr and O. M. Faltinsen, A B-spline based BEM for unsteady free-surface flows. *J. Ship Res.* 43 (1999) 1–12.
51. F. Solaas, *Analytical and Numerical Studies of Sloshing in Tanks*. Ph.D. thesis. Trondheim: Dept. Marine Hydrodynamics NTNU (1995) 216 pp.
52. Y. Kim, Numerical simulation of sloshing flows with impact load. *Appl. Oce. Res.* 23 (2001) 53–62.
53. N. E. Mikelis, J. K. Miller and K. V. Taylor, Sloshing in partially filled liquid tanks and its effect in ship motions. *Numerical simulation and experimental verification*. RINA Spring Meeting (1984) pp. 267–281.

54. J. Kvaalsvold, *Hydroelastic Modelling of Wetdeck Slamming*. Ph.D. Thesis. Trondheim: Dept. Marine Hydrodynamics NTNU (1994) 172 pp.
55. O. M. Faltinsen, O. F. Rognebakke, I. A. Lukovsky and A. N. Timokha, Multidimensional modal analysis of nonlinear sloshing in a rectangular tank with finite water depth. *J. Fluid Mech.* 407 (2000) 201–234.
56. O. M. Faltinsen and A. N. Timokha, Adaptive multi-modal approach to nonlinear sloshing in a rectangular tank. *J. Fluid Mech.* 432 (2001) 167–200.
57. O. M. Faltinsen and A. N. Timokha, Asymptotic modal approximation of nonlinear resonant sloshing in a rectangular tank with small fluid depth. *J. Fluid Mech.* 470 (2001) 319–357.
58. O. M. Faltinsen, O. F. Rognebakke and A. N. Timokha, Resonant three-dimensional nonlinear sloshing in a square-base tank. *J. Fluid Mech.* 487 (2003) 1–42.
59. O. F. Rognebakke and O. M. Faltinsen, Damping of sloshing due to tank roof impact. In: *15th Int. Work. on Water Waves and Floating Bodies*. Caesarea (2000) pp. 158–161.
60. O. M. Faltinsen, Slamming on ships. In: P. Cassella, A. Scamardella and G. Festinese (eds.) *Proc. IX Congress IMAM International Maritime Association of Mediterranean*. Ischia I (2000) pp. 25–36.